CHARACTERIZATION OF A NINTENDO WII

FOR TRACKING A HAPTIC GLOVE IN 3D

By

Graham Clark Kryger

A thesis submitted in partial fulfillment
of the requirements for the degree of

MASTER OF SCIENCE IN MECHANICAL ENGINEERING

WASHINGTON STATE UNIVERSITY
School of Engineering and Computer Science, Vancouver

December 2009

To the Faculty of Washington State University Vancouver:

To the members of the Committee appointed to examine the thesis of GRAHAM CLARK KRYGER finds it satisfactory and recommends that it be accepted.

Hakan Gurocak, Ph. D., (Chair)

Linda Chen, Ph. D.

Wei Xue, Ph. D.

ACKNOWLEDGMENT

From the start of this project to the end, there are several persons who have assisted in the progress of my thesis over the last two years. I could not have completed it without their invaluable help.

I would first like to thank my advisor, Dr. Hakan Gurocak, from whom I have learned so much. The guidance, knowledge, and advice he has imparted to my master's study have been phenomenal. I am much more enriched and accomplished because of his support.

The second person I am grateful to is Dr. Dave (Dae-Wook) Kim for his methods of optimization which were used for the MR brake dimensions.

I would like to thank Chad Swanson and Troy Dunmire for their time and advice with the manufacturing of the many parts needed throughout these last couple years.

For all those who volunteered their time for the experiments I undertook, I would like to also show my appreciation. To my fellow graduate students, thank you for the encouragement and company you have provided.

Lastly, I want to thank my father, mother and three brothers for their dedication, encouragement, and unending support.

CHARACTERIZATION OF A NINTENDO WII

FOR TRACKING A HAPTIC GLOVE IN 3D

Abstract

by Graham Clark Kryger, M.S.
Washington State University
December 2009

Chair: Dr. Hakan Gurocak

The long-term goal of our research is to develop a lightweight and powerful haptic glove. The main challenge in achieving this goal is the development of actuators that are small enough to be placed on the hand, yet powerful enough to restrict or stop the motion of the fingers as the user grasps a virtual object. Another challenge is the real-time measurement of the position and orientation of the user's hand in 3D. Current devices, such as the Flock of Birds sensors, are very expensive. They also restrict the user's movement with long cables and the need to be near an electromagnet for the sensors to measure positions.

In this research, the objectives were (1) to explore the possibility of using the Nintendo Wii Remote as an inexpensive position/orientation measurement system to track the user's hand, and (2) to

explore the design of a small actuator using magnetorheological fluid and a permanent magnet. The research contained three phases: characterization of the Nintendo Wii Remote, design of a lightweight haptic glove, and design of a small actuator.

The performance of the Wii Remote in measuring position and orientation in 3D was characterized through experiments with one and two cameras and by using a Coordinate Measurement Machine (CMM). It was found that the two-parallel-cameras arrangement yielded the best measurement accuracy in about 50 cm depth from the cameras. The work volume at this depth was optimized by adjusting the camera angles and LED targets to create an optimized 3D space for tracking the user's hand motion with the best accuracy.

The research also explored conceptual design of a lightweight haptic glove and a small actuator. CAD model of the glove was developed by introducing improvements over the existing glove designs in our laboratory.

Conceptual design of an actuator was completed. It uses magnetorheological (MR) fluid, a permanent magnet and a small motor to provide variable resistance forces to motion. It is envisioned that such small actuators will be implemented in a future haptic glove to provide a more realistic virtual reality simulation environment.

TABLE OF CONTENTS

LIST OF FIGURES

LIST OF TABLES

Dedication

This thesis is dedicated to
my father, mother, and three brothers.

CHAPTER 1

INTRODUCTION

One of the newest applications with computers is interacting with virtual objects. One application for this tool, often termed virtual reality (VR), can allow the testing of equipment prior to manufacturing and long distance medical procedures through a robotic surrogate. To correctly simulate a virtual environment several constructs must be present. These requirements may consist of tracking objects through 3D space, user interface design through a haptic glove, and force generation.

1.1. 3D Tracking

There are several techniques for tracking the movements of the user. Most systems today use a linkage system to gather the position and moments of an individual [1]. Newer systems are wireless and gather that information indirectly. One method uses Cameras with a filter. When calibrated, these Cameras can locate specific light sources and triangulate a point in space. Conveniently, this is relatively inexpensive and requires little time to setup. Another process uses a magnetic field and a sensor to detect the changing magnetic flux. This alternative can be extremely precise but has a drawback requiring cables and a high cost.

Using the first method with Cameras, the primary limitation is the resolution that the Camera can provide. The greater the detail, the more precise the triangulation will be. The concept spawned by Johnny Chung Lee's project [2], uses a readily available product. This product, now marketed as the Nintendo Wii Remote, has a Camera to track up to four IR light sources. Where the Nintendo Wii

Console uses a movable Wii Remote and a fixed light bar as a point of reference, Lee's projects reversed the roles by using stationary Wii Remotes to track moving LED light sources.

Several attempts have been made to use Lee's concept for VR simulations. One idea outlined by Yang-Wai Chow used two Nintendo Wii Remotes. The first was mounted on the ceiling, while the other was used like a wand. Two IR light sources were mounted on both ends of the moveable Wii Remote. Under these conditions, the Wii Remote on the ceiling acted to provide the location and yaw angle of the second Wii Remote, while the second returned the roll and pitch calculations of itself to the computer. In his computer game, the movable Wii Remote acted as a gun, and targets were to be shot. Based on the methodology, the goal was not how precise the system could measure the angles, but how accurate a person could align the Wii Remote with the center of a target [3].

One of the best sources available on the Wii Remote is a Master's thesis [4]. This research indicated that if an IR source was unavailable, the Camera would track any bright object. The capabilities of the Wii Remote were tested. In our research, we tested similar capabilities but used a very high precision CMM. A metric, called "Freedom of Movement," was defined as an indicator of the available workspace to a user. We incorporated the same terminology within our experiments.

1.2. User Interface

One option for effective user VR interface is through the use of a haptic glove. A crucial factor in glove design is that the features conform to the user's hand. Conrad Bullion, a graduate student in the Mechanical Engineering program at Washington State University Vancouver, developed an effective glove design that used a linkage system by enabling the bending of the finger joints to move as one. This design represented a good starting point for use because it reduced the number of sensors and actuators necessary from three to one per finger [5].

1.3. Force Generation

There are several methods for generating a force which results in a sensation of pressure that a user can feel. These methods include pneumatics, motors, and magnetorheological (MR) brakes.

Pneumatics is a growing field of research. When applied to haptics, size is often the critical factor. Pneumatic muscles are available to fulfill the size requirement. However, to control these muscles, additional hardware and complex control algorithms are required. It is often bulky and can be quite costly. A pressurized air source is also required, removing any wireless capabilities [6].

Goktug Dazkir, a graduate student in Mechanical Engineering program at Washington State University Vancouver, explored the use of motors aligned with strain gauges for accurate force measurements. This method worked fairly well but required extensive electronic circuits and software design [7].

At Washington State University Vancouver, our primary focus in force generation has been on design of radial MR brakes. These devices were created on a very small scale with typical sizes of about 1” in diameter. Each design worked under the principle of creating a serpentine pathway for the magnetic flux to pass through the MR fluid to maximize the force generated. In this research, we opted for a linear MR Brake design. Typical designs were similar to a shaft and piston schematic. Design of a compact linear MR brake is a challenge [8].

CHAPTER 2

PROBLEM STATEMENT AND SCOPE OF RESEARCH

In a Virtual Reality (VR) simulation environment, providing realism to the user is a crucial and challenging task. Ideally, it needs to be done in such a way that the user is unaware that he/she is immersed in a virtual world. There is a concerted effort in the research community to improve the reality of VR environments from several aspects. One of these facets is providing the user with the sensation of interacting with objects through touch and force feedback. Special user interfaces, called haptic interfaces, enable the user to feel various material properties such as weight, stiffness and texture of a virtual object. These interfaces may have many applications in telerobotics, medical training, and product development. An important interface is the haptic glove. It opens up the world of force feedback by allowing the user to pick up and feel virtual objects in a much more natural way. The literature surrounding this research contains many examples. In almost all of these devices, a remote box houses a large number of actuators and sensors. Power to the glove is transmitted via cables.

The long-term goal of our research is to develop a lightweight and powerful glove. The main challenge in achieving this goal is the development of actuators that are small enough to be placed on the hand, yet powerful enough to restrict or stop the motion of the fingers as the user grasps a virtual object. Another challenge is the real-time measurement of the position and orientation of the user's hand in 3D. Current devices, such as the Flock of Birds sensors, are very expensive. They also restrict

the user's movement with long cables and the need to be near an electromagnet for the sensors to measure positions.

In this research, the objectives were (1) to explore the possibility of using the Nintendo Wii Remote as an inexpensive position/orientation measurement system to track the user's hand, and (2) to explore the design of a small actuator using magnetorheological fluid and a permanent magnet. The research contains three phases: characterization of the Nintendo Wii Remote, design of a lightweight haptic glove, and design of a small actuator.

2.1. Characterization of the Nintendo Wii Remote

This phase of the research characterizes the Wii Remote to explore how large a workspace can accurately be measured using the Wii Remote for 3D hand tracking for VR applications. The following experiments were conducted using a Coordinate Measuring Machine (CMM) to quantify the accuracy of the position/orientation measurements of the Wii Remote.

<u>Using One Camera</u>

1. Determine the vertical and horizontal viewing angles of a Wii
2. Determine the minimum and maximum distance (depth) that can reliably be measured within the workspace
3. Determine the accuracy of roll angle measurements
4. Determine Camera sensitivity

<u>Using Two Parallel Cameras</u>

1. Determine the impact of the angle of inclination of the infrared LED targets on the measurements by the Wii Remote

2. Determine the minimum and maximum distance (depth) that can reliably be measured within the workspace
3. Determine the accuracy of roll, pitch and yaw angle measurements
4. Using the "Freedom of Movement" metric, determine the size of the workspace with the most accurate and reliable measurements

The research then explored a two-camera setting with the Cameras turned towards each other to determine if the size of the work volume could be increased in the region where the most accurate measurements were obtained from the Wii Remote.

2.2. Design of a Lightweight Haptic Glove

This phase of the research involved initial design of a future glove that would accommodate the small actuators and the LED targets of the Wii Remote for hand position/orientation measurements in 3D. An initial CAD model of the glove was developed.

2.3. Design of a Small Actuator

In this phase of the research, a small actuator was designed. The actuator uses magnetorheological (MR) fluid, a permanent magnet and a small motor. The ultimate goal is to use these actuators in the implementation of a future haptic glove. The steps below were followed.

1. Design the actuator and create a Finite Element Method (FEM) for analysis
2. Using this model along with ANOVA statistical method, determine the most sensitive parameters of the design
3. Optimize the design by selecting the best values for the sensitive parameters while keeping the actuator size compact and output power high
4. Produce CAD models of the actuator for future fabrication and use in the haptic glove

CHAPTER 3

CHARACTERIZATION OF THE WII REMOTE

One of the challenges in designing a lightweight haptic glove is the real-time measurement of the position and orientation of the user's hand in 3D. Current devices, such as the Flock of Bird sensors, are very expensive. They also restrict the user's movement with long cables and the need to be near an electromagnet for the sensor to measure positions. The Nintendo Wii Remote is an inexpensive alternative. In this approach, a small target with 3 infrared LEDs can be placed on the hand of the user. The Nintendo Wii Remote Camera placed on or near the computer monitor can then track the motion of the hand as the user interacts with the virtual world displayed on the screen. In this chapter, we explore how large a workspace can accurately be measured using the Wii Remote for 3D hand tracking for VR applications.

3.1. Wii Schematics

The Nintendo Wii introduced a new innovation with console games. By enabling a fully interactive device, the Wii Remote can sense relative position using the Wii Sensor Bar and an accelerometer inside the Remote. In addition, the Wii Remote and the Numchuk accessory are capable of pitch, roll and 3-D acceleration detection.

Wii Remote Numchuk Wii Sensor Bar

Figure 3.1
Wii Devices [9]

When using the Nintendo Wii Remote as a tracking system, there are a few things to consider. The first is that the Wii Remote Camera can only detect infrared light. This is convenient because the image will contain the tracking object without a background. The second consideration is that the field of view is limited. To increase this limitation, a lens needs to be inserted between the path of the Camera and the target. For our purposes, a lens will not be used.

3.2. Tracking Schemes

Within the Nintendo Wii system, the direction that the Wii Remote is pointing is based on the two LED light groups that are located on either end within the Wii Sensor Bar. The Camera located behind the black infrared filter on the front of the Wii Remote takes the 2D image, measures the intensity of each point, calculates the distance between each point, and determines the location of each point. If the Wii Remote moves closer to the Wii Sensor Bar, the Camera determines that the intensity of each point increases as well as the distance between each point. Thus, the computer knows that the Wii Remote has moved forward. The same principle applies when rotating the Wii Remote away from or towards the Wii Sensor Bar.

Tracking an object in 3D space is a little more complicated than the relative movement as described above. This thesis tried to design a tracking system that can determine the position as well as tilt, roll, and yaw.

3.2.1. Two Perpendicular Wii Remotes

As shown in Figure 3.2, tracking an object in 3D space can be achieved using two Remotes where one Remote can track the position and the other deals with the tilt and roll [3]. However, this method adds a lot of mass to the glove.

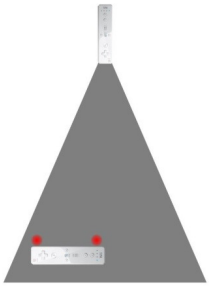

Figure 3.2
Tracking with Wii Remote [3].

3.2.2. Stereo Tracking with Two Parallel Wii Remotes

In this approach, there are two fixed Wii Remotes that are separated by a distance (Figure 3.3). The two Cameras can determine the tilt and roll of the LED tracking object. However, the accuracy is determined by the resolution of the image [4].

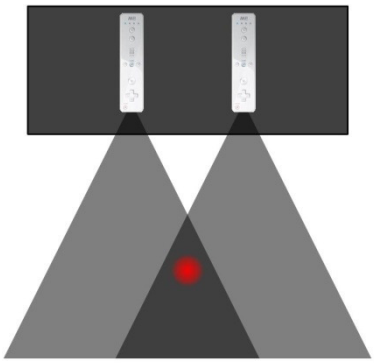

Figure 3.3
Tracking with Two Parallel Wii Remotes

3.2.3. Tracking with One Wii Remote

An approach suggested by Wimmer, Boring, and Müller, uses one Wii Remote and is shown in Figure 3.4 [10]. Initial analysis discovered a problem in that the Wii Remote tracks up to four infrared light sources and the light source has eight. This design was not tested.

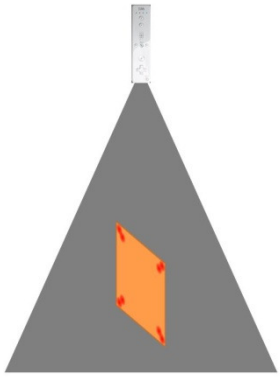

Figure 3.4
Tracking with One Wii Remote [10].

3.3. Measurement Setup

In this research, a Coordinate Measurement Machine (CMM) was used to measure target object locations with high precision. Our CMM is a small table-top unit with a work volume of 463 mm (x plane), 512 mm (y plane), and 365 mm (z plane). Because the work volume is smaller than the volume needed to be measured, an add-on platform was fabricated to facilitate an expanded volume. Figure 3.7 shows the extension platform and the coordinate frame orientations for the Wii Remote and the CMM.

For additional consistency throughout of the entire test, the axis of orientation of the CMM was used instead of the orientation of the Wii Remotes. See Figure 3.5 and Figure 3.6 for axis orientation comparison.

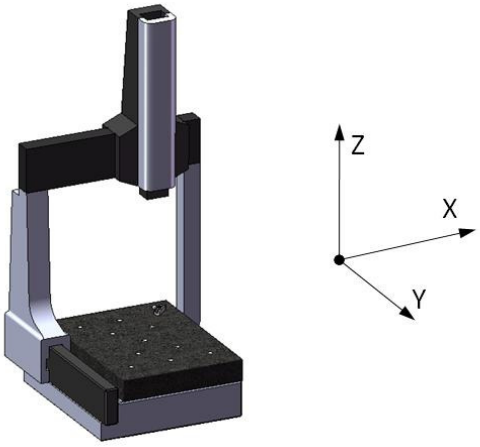

Figure 3.5
CMM Axis Orientation

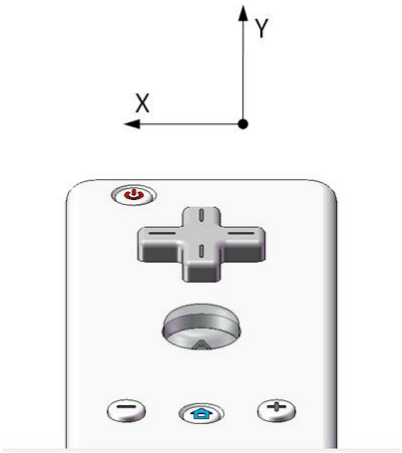

Figure 3.6
Wii Remote Axis Orientation

The extension platform was constructed using aluminum structural elements. Brackets were fastened in increments of 250 mm for the Wii Remotes' platform to be positioned against and then clamped down. These brackets were positioned on the platform accurately by using the CMM. Precise dimensions of the extension platform are shown in Figure 3.11.

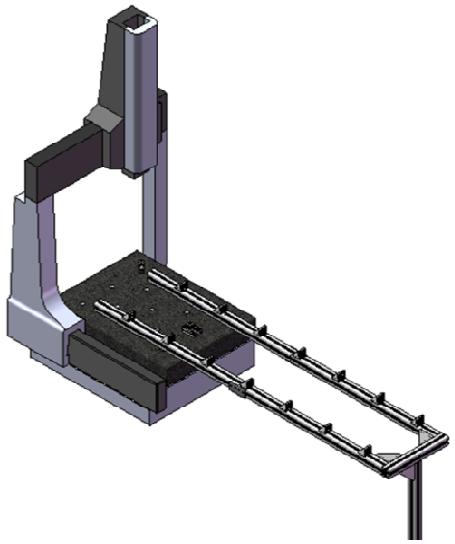

Figure 3.7a
Extended Platform

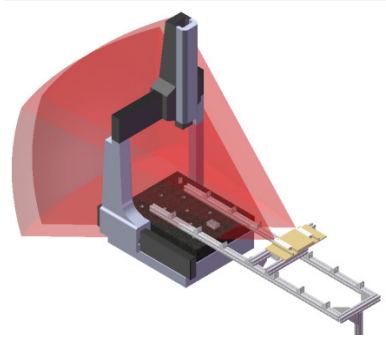

Figure 3.8b
Measuring Setup using a CMM

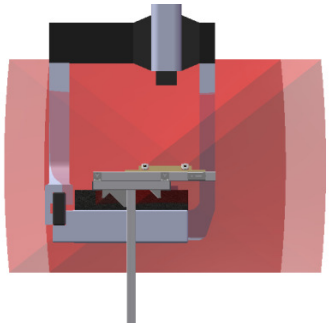

Figure 3.9c
Front View

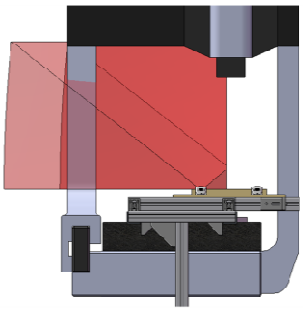

Figure 3.10d
Scanning Volume

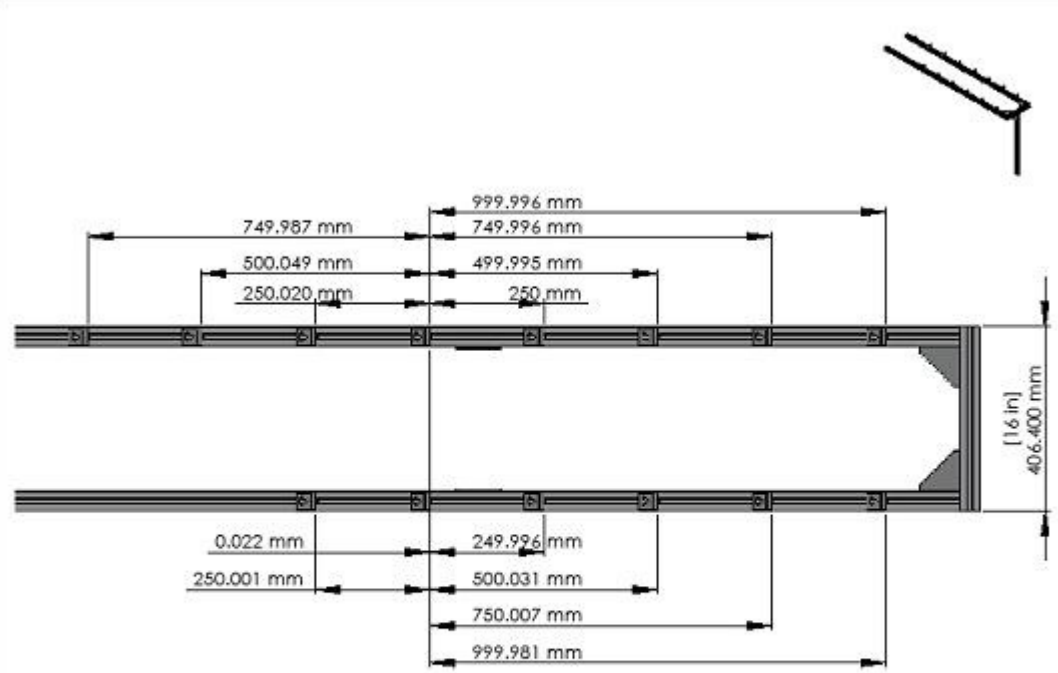

Figure 3.11
Main Frame Measured Calibration

The Wii Remotes were mounted on a base. Two different settings were used in the experiments as shown in Figure 3.12 and Figure 3.13.

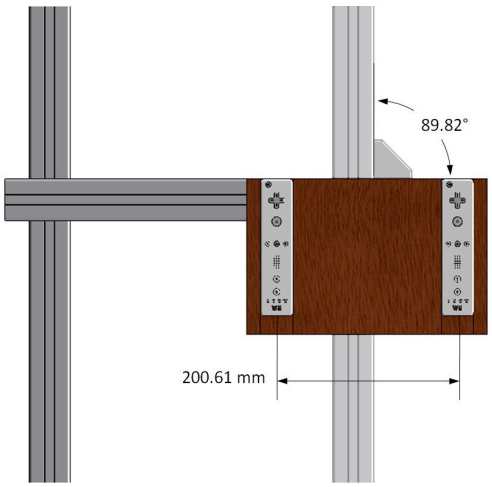

Figure 3.12
Wii Platform Measured Calibration
Experiment Sets 1 and 2

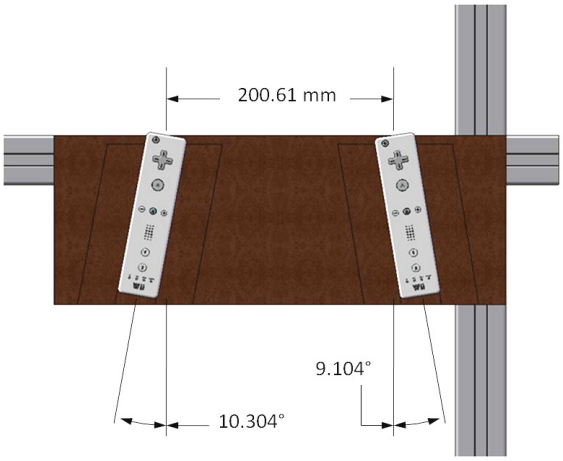

Figure 3.13
Wii Platform Measured Calibration
Experiment Set 3

Two different sizes of targets were made out of Plexiglas. The first design (Figure 3.14) was used in the first set of experiments. It held two infrared LEDs, a resistor, a switch and a battery. The second design (Figure 3.15) was made smaller to more closely resemble the type of target that would be mounted on a haptic glove. This second setup was used in the second and third sets of experiments.

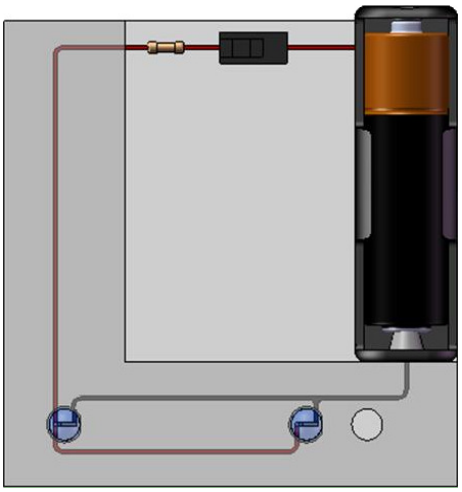

Figure 3.14
LED Mount
Experiment Set 1

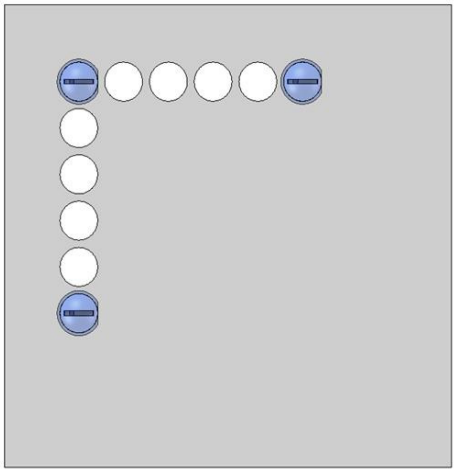

Figure 3.15
LED Mount
Experiment Sets 2 and 3

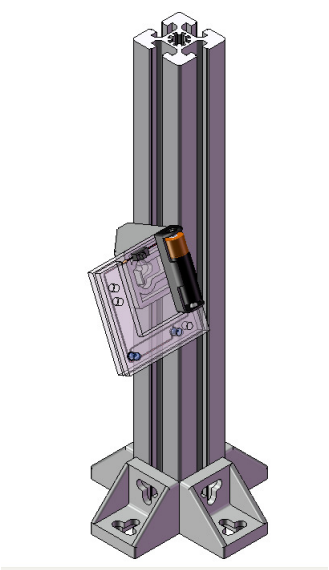

Figure 3.16
LED Mount Attached
Experiment Set 1

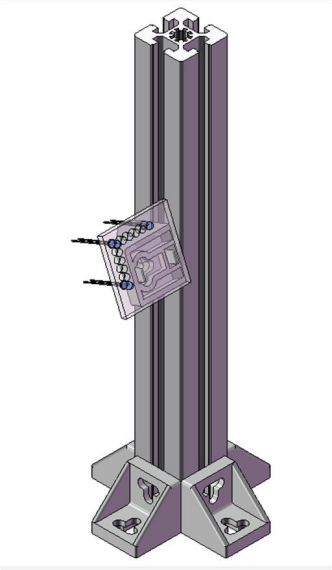

Figure 3.17
LED Mount Attached
Experiment Sets 2 and 3

3.4. Software Interface for the Wii Remotes

The Wii Remotes communicate with a computer using Bluetooth technology. We purchased a Bluetooth USB dongle by BlueSoleil [11] recommended for the Wii applications to act as the transmitter and receiver. Using the software provided by the dongle, two Wii Remotes could easily be interfaced to the computer (Figure 3.18 and Figure 3.19).

To interpret the output data from the Remotes, two programs were used. The "*Wii Remote Sandbox"* [12] was used to gather relative information (Figure 3.19). This program had limited IR sensor information. For retrieving the IR sensor locations, a program provided by "*WiiYourself*" [13] was used. It provided similar data to that of the previous program but in a Command Prompt Interface (Figure 3.20). This latter software was modified to show more increased precision for the IR locations. The code modification is shown in Appendix B.

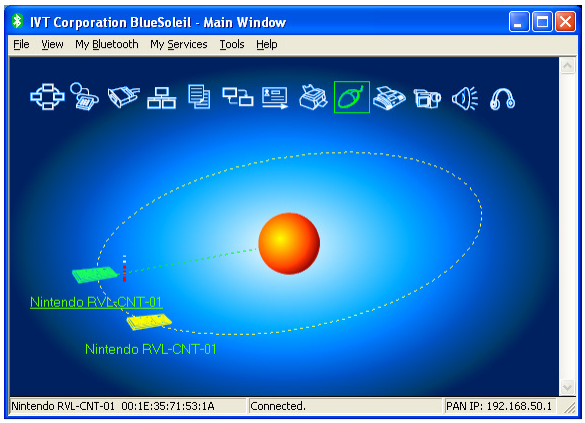

Figure 3.18
BlueSoleil Bluetooth Connecting Software

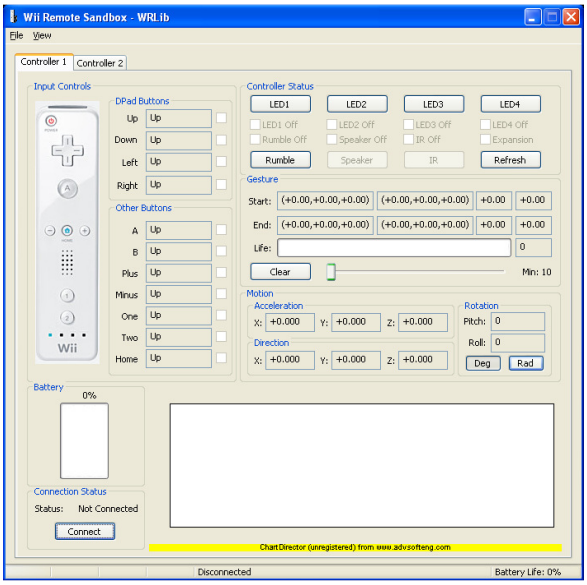

Figure 3.19
Wii Remote Sandbox Software

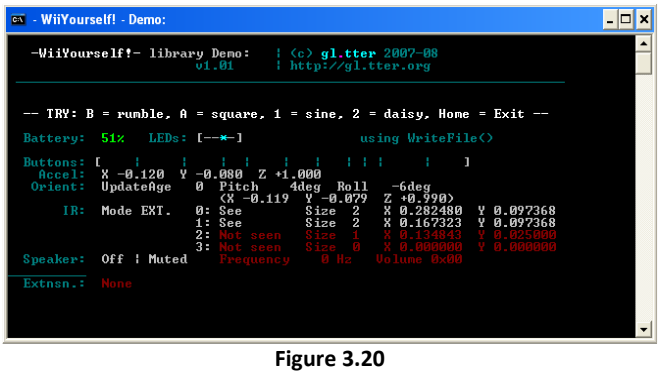

Figure 3.20
WiiYourself Software

3.5. Experiments

To accurately measure the characteristics of the Wii Remote, three sets of experiments were designed: (1) One Wii Remote, (2) Two Parallel Wii Remotes, and (3) Two Angled Wii Remotes.

3.5.1. One Wii Remote

This set of experiments was used to find the capabilities of a single Wii Remote using the simplest conditions.

3.5.1.1. Experiment 1.1: Lens Spread

For this test, the measurements were taken on all edges of the Wii Remote view. The goal was to determine the angle at which the original manufacturer's lens on the Remote detects the infrared light from the LED source. Figure 3.21 and Figure 3.22 show the data points collected along the edges of the Camera view. The relative angles of the lines are noted in the legend.

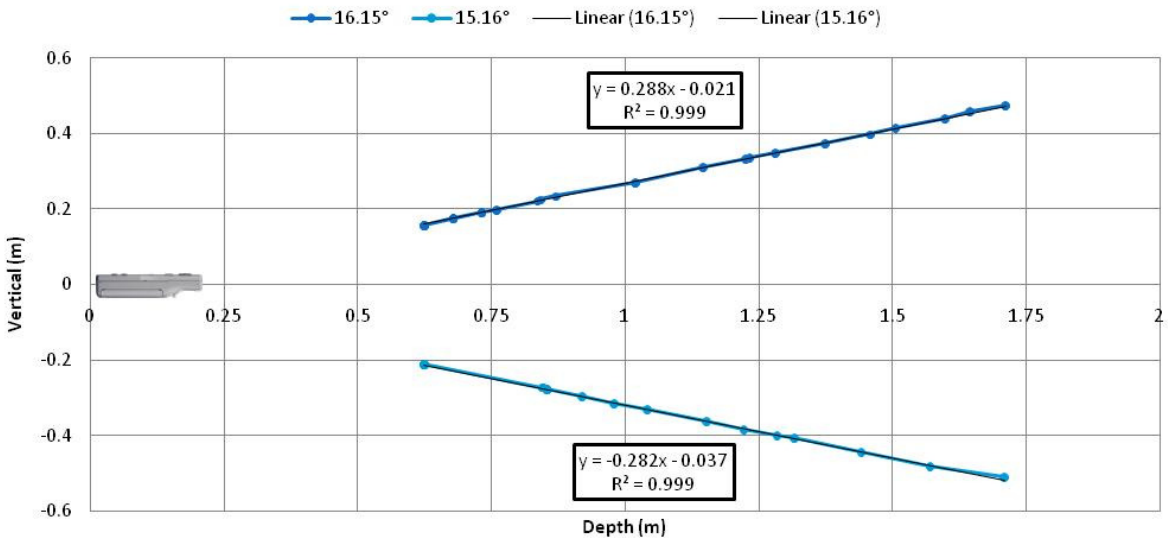

Figure 3.21
Vertical Edge Interface vs. Depth from Camera

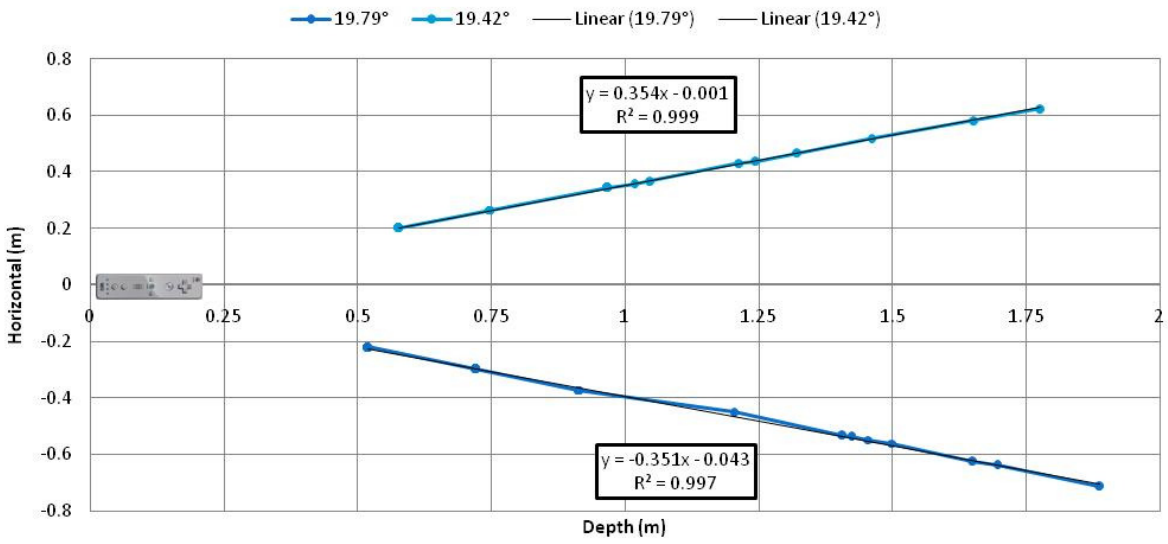

Figure 3.22
Horizontal Edge Interface vs. Depth from Camera

During the experiment, it was found that making adjustments in the horizontal plane was much easier than that in the vertical plane. Minute translations in the X or Y plane necessitated sliding the stand which supported the LEDs. However, the Z plane adjustment meant loosening a bolt and adjusting the entire assembly. A solution to this problem was found in simply adjusting the height of the LED to a value near what was needed. Then, the depth of the stand was adjusted in the Y plane (Figure 3.7) until the LED crossed the viewing plane, and the correct Wii LED location was measured using the CMM.

The measurements showed that there was a vertical spreading angle of 31.31° and a horizontal spreading angle of 39.21°. These numbers were very similar to the results reported in [4] as 31° and 41°, respectively.

Because of the support structures mounted to the CMM, we were unable to make regular interval measurements. This will explain the irregular spacing between the upper and lower lines on the previous charts. The intervals were adjusted to 250 mm as shown in the following Experiment Sets.

3.5.1.2. Experiment 1.2: Camera Sensitivity

The goal of this experiment was to find the size of the Camera's pixels in the horizontal axis to assess the sensitivity of the Remote's Camera. Measurements were first taken to determine how much physical movement in the target position would cause a single pixel change in the Camera's reading. However, this turned out to be very difficult to measure reliably. To increase the accuracy, we moved the target until a 10-pixel difference was registered. Later, the distance through which the target moved was divided by ten to obtain the average change per pixel. The sensitivity at the center of the Camera view was slightly higher than that of the outer regions (Figure 3.23 and Figure 3.24).

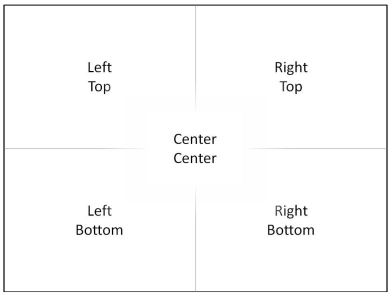

Figure 3.23
Measured Pixel Locations

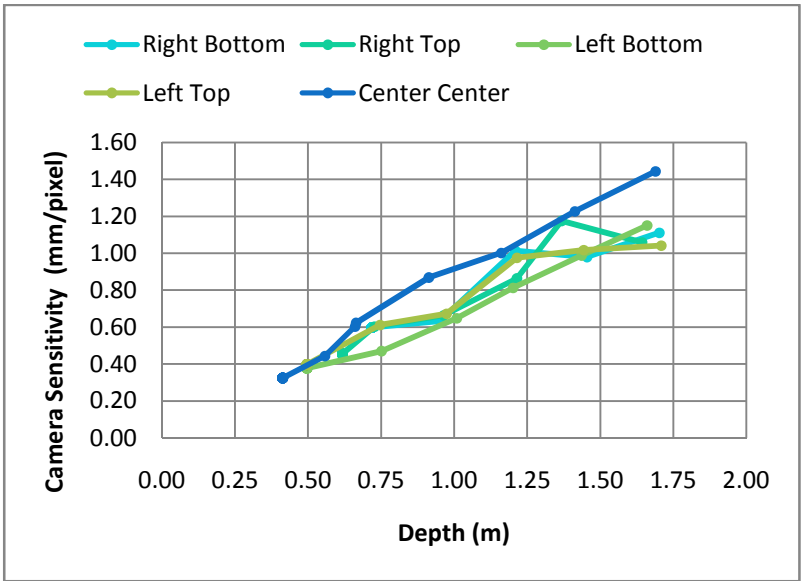

Figure 3.24
Camera Sensitivity vs. Depth from the Camera

3.5.1.3. Experiment 1.3: Roll Angle

The goal of this experiment was to measure the accuracy of the roll angle of the target reported by the Wii Remote. The two LEDs on the target were activated. The CMM was used to locate the center of the LEDs, and a planer angle was calculated (Figure 3.16). To make the data more systematic, the location of the stand and angular increments were set at 250 mm and 15°. This was chosen because there were no obstacles to prevent its placement. Once the stand and block were placed and measured, the Wii Remote was moved to a depth of 1750 mm from the IR LEDs. The results are seen in Figure 3.25.

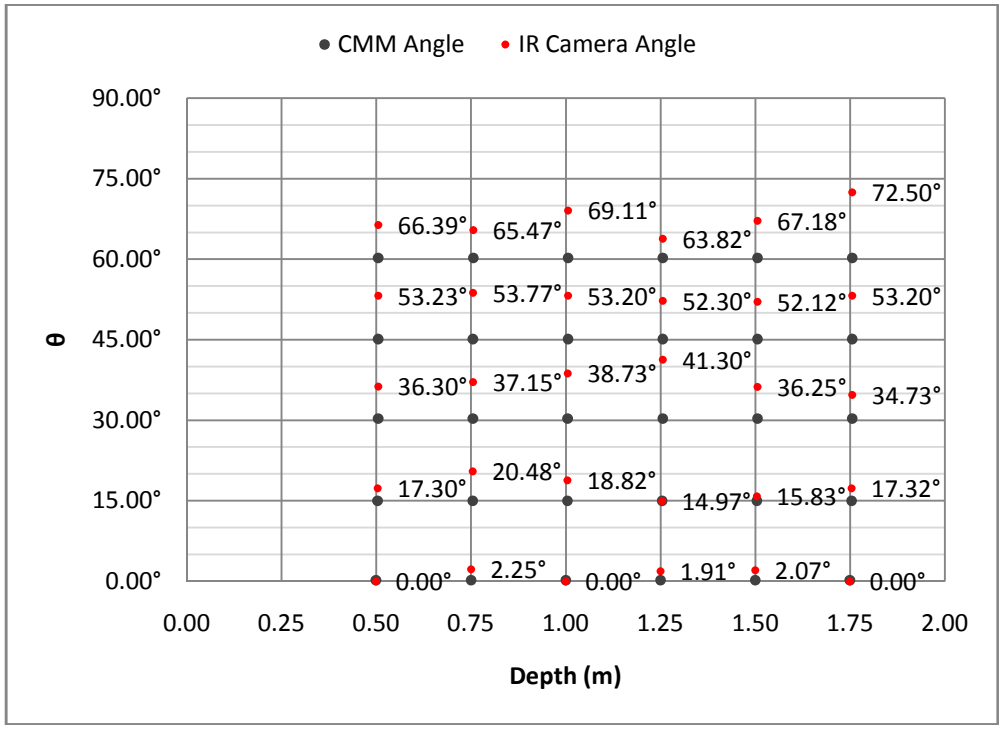

Figure 3.25
Measured Angle vs. Depth from Camera

3.5.1.4. Experiment 1.4: Depth Analysis

In this experiment, the goal was to determine the minimum and maximum depth along the line of the Camera that the Wii Remote could detect. For this information, the data used was from the previous three experiments. The IR point location was combined with the measured depth to the

Camera. The slopes and intercepts used in these equations were from Experiment 1.1 data as shown in Table 3.1.

Variable	Value
$X_{Slope\ 1}$	-0.3513067
$X_{Slope\ 2}$	0.3548103
$X_{Y\ Int\ 1}$	-0.0431398
$X_{Y\ Int\ 2}$	-0.0018957

Variable	Value
$Z_{Slope\ 1}$	-0.2819836
$Z_{Slope\ 2}$	0.28869
$Z_{Y\ Int\ 1}$	-0.0199013
$Z_{Y\ Int\ 2}$	-0.034689

Table 3.1
Wii Experiment 1.4 Variables

Translation of the data point along X-axis was computed using:

$$X = X_{ir} \cdot \left(\left(X_{Slope\ 2} - X_{Slope\ 1} \right) \cdot Y + \left(X_{Y\ Int\ 2} - X_{Y\ Int\ 1} \right) \right) + \left(\left(X_{Slope\ 1} \right) \cdot Y + \left(X_{Y\ Int\ 1} \right) \right) \quad \textbf{(3.1)}$$

Translation of the data point along Z-axis was computed using:

$$Z = Y_{ir} \cdot \left(\left(Z_{Slope\ 2} - Z_{Slope\ 1} \right) \cdot Y + \left(Z_{Y\ Int\ 2} - Z_{Y\ Int\ 1} \right) \right) + \left(\left(Z_{Slope\ 1} \right) \cdot Y + \left(Z_{Y\ Int\ 1} \right) \right) \quad \textbf{(3.2)}$$

In Figure 3.26 and Figure 3.27, the black data points represent the CMM measured locations and the bars represent the error associated in the calculation with the Wii IR Camera.

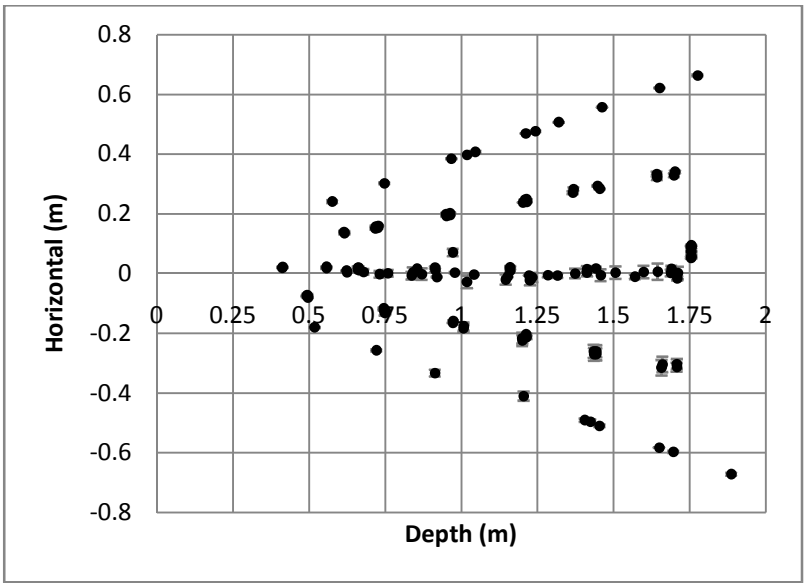

Figure 3.26
Horizontal Measured Location vs. IR Camera Location

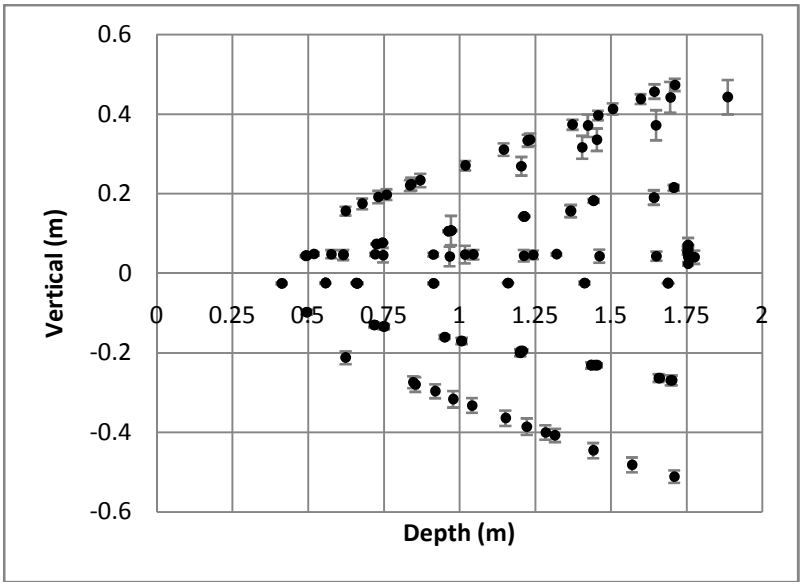

Figure 3.27
Vertical Measured Location vs. IR Camera Location

In Figure 3.28 and Figure 3.29, the difference between the CMM measured location and the measured Wii Camera location are displayed. As expected, the error tends to increase as the depth from the Camera gets larger. With the horizontal distribution, it has a shift towards the left, where positive is on the right and negative is on the left. Also, the vertical distribution is more even above and below the axis.

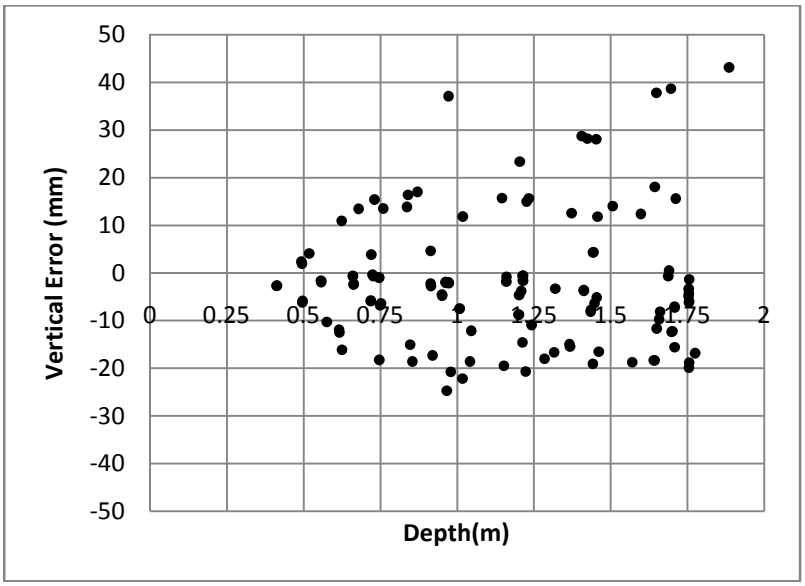

Figure 3.28
Vertical Error vs. Depth from Camera

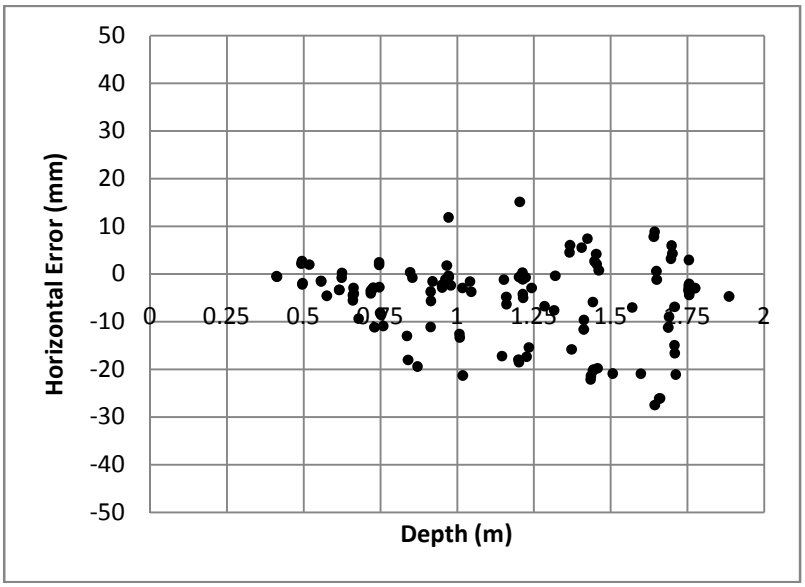

Figure 3.29
Horizontal Error vs. Depth from Camera

3.5.2. Two Parallel Wii Remotes

For these experiments a smaller version of the target was developed (Figure 3.15). As the optimum distance between LEDs was unknown, several holes were drilled into a small sheet of Plexiglas so that their distances could be adjusted as needed. The primary concern was that placing them too close would cause the Wii Remote Camera to misinterpret two IR lights as one. The results of Experiment 1.2 indicated that less than 2 mm physical distance between the LEDs would trigger a change in the pixel readings which was less than the 2.5 mm radius of the LEDs we used. Therefore, even if the LEDs were adjacent to each other, no mistaken measurements would occur.

3.5.2.1 Experiment 2.1: LED Angle of Inclination

Throughout the first set of experiments, it was observed that the angle that the IR LED pointed relative to the Wii Remote was very important. In this experiment, the effect of the angle of inclination on the Camera's ability to make a measurement was investigated. Table 3.2 shows manufacturer's data for the Radio Shack model 276-0143 LEDs we used.

Electric characteristic	25° C	**Radiant power output**	16 mW min. (100 mA)
Viewing angle to ½ intensity	45°	**Forward voltage**	1.2 V
Wavelength	940 nm	**Forward current**	100 mA

Table 3.2
LED Characteristics of Radio Shack Model 276-0143

One significant observation was that the closer the IR LED was moved to the Wii Remote Camera, the closer the LED lens spreading angle approached the 45° value that was recorded in Table 3.2 (Figure 3.30 and Figure 3.31). Keeping the vertical height constant, the angle was tested at a variety of locations. In Figure 3.30, the X axis is scaled in pixels to remove the depth variable.

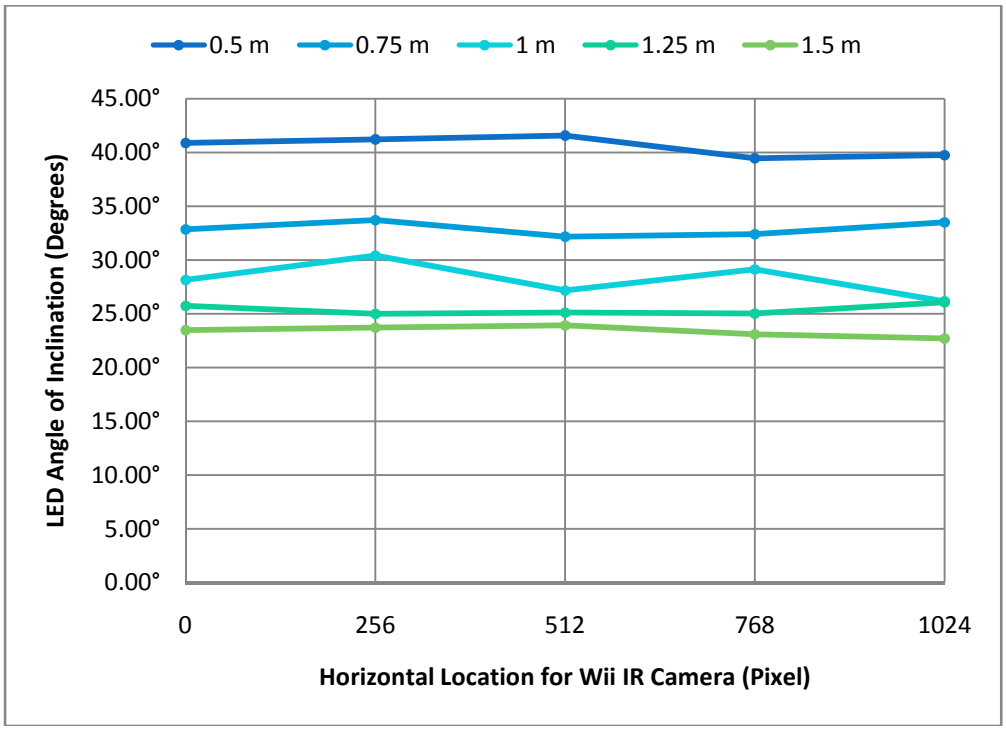

Figure 3.30
LED Angle vs. Wii Remote Camera Location

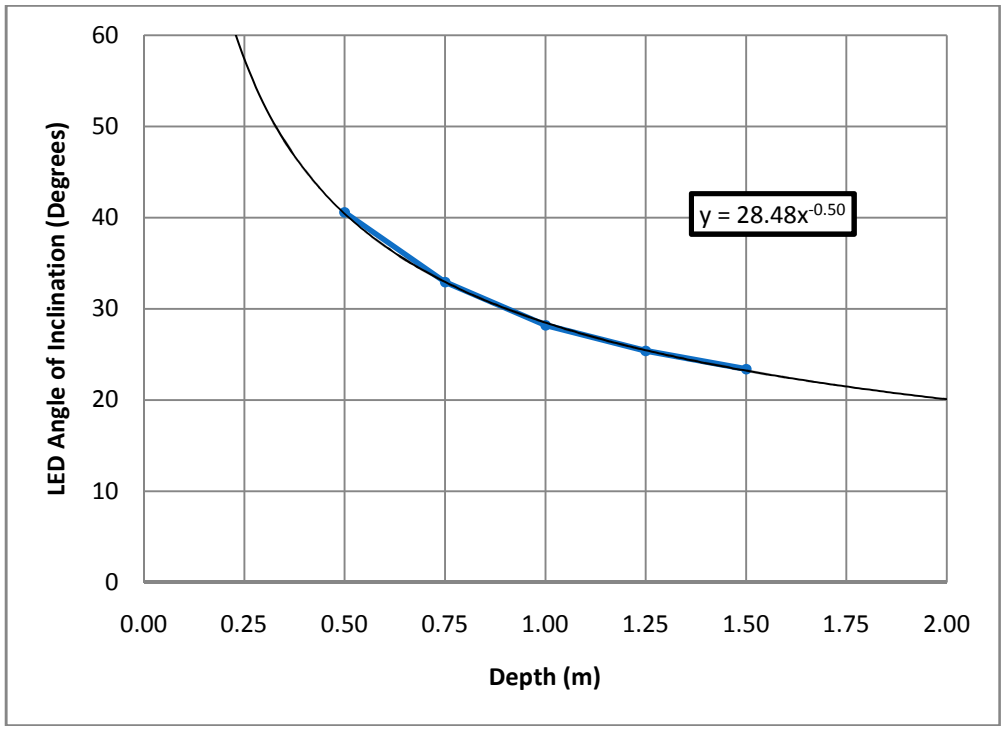

Figure 3.31
LED Angle vs. Depth from Camera

3.5.2.2 Experiment 2.2: Depth Analysis

This analysis, being similar to Experiment 1.4, dealt more with the 3D locations. An initial distance which was required in that test was not needed here. To calculate the positions, the following geometric references and equations were used (Figure 3.32, Figure 3.33, and Equations (3.3) through (3.10)).

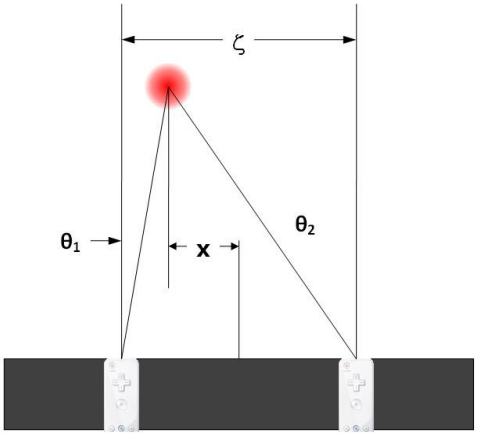

Figure 3.32
Dimensions and Variables
Top View

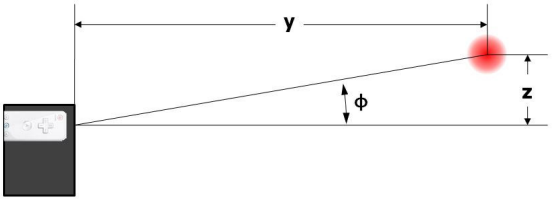

Figure 3.33
Dimensions and Variables
Side View

The manufacturer's spreading angles of 41° and 31° will be used instead of the values found in Experiment 1.1.

Horizontal and Vertical Angle Scalars

$$\boldsymbol{h = tan\left(\frac{\frac{41^\circ}{2}}{\frac{1.0}{2}}\right)} \quad \textbf{(3.3)}$$

$$\boldsymbol{v = tan\left(\frac{\frac{31^\circ}{2}}{\frac{1.0}{2}}\right)} \quad \textbf{(3.4)}$$

For the Wii Remote Camera, an object directly ahead appeared with the location 0.5 (0.0 minimum, 1.0 maximum). To correct this in Equations (3.5) through (3.7), $(0.5 - X_1)$, $(0.5 - X_2)$, and $(Y_2 - 0.5)$ were used.

Angle Calculations

$$\boldsymbol{\theta_1 = tan^{-1}\big((0.5 - X_1) * h\big)} \quad \textbf{(3.5)}$$

$$\boldsymbol{\theta_2 = tan^{-1}\big((0.5 - X_2) * h\big)} \quad \textbf{(3.6)}$$

$$\boldsymbol{\Phi = tan^{-1}\big((Y_2 - 0.5) * v\big)} \quad \textbf{(3.7)}$$

Cartesian Coordinate Equations

$$\boldsymbol{y = \frac{\varsigma}{tan(\theta_1) - tan(\theta_2)}} \quad \textbf{(3.8)}$$

$$\boldsymbol{x = -\frac{\varsigma}{2} + z * tan(\theta_1)} \quad \textbf{(3.9)}$$

$$\boldsymbol{z = y * tan(\Phi)} \quad \textbf{(3.10)}$$

As seen in Figure 3.34, Figure 3.35, and Figure 3.36, there was very little error in the depth from the LED to the Wii Remote. However, the error was primarily in the horizontal axis.

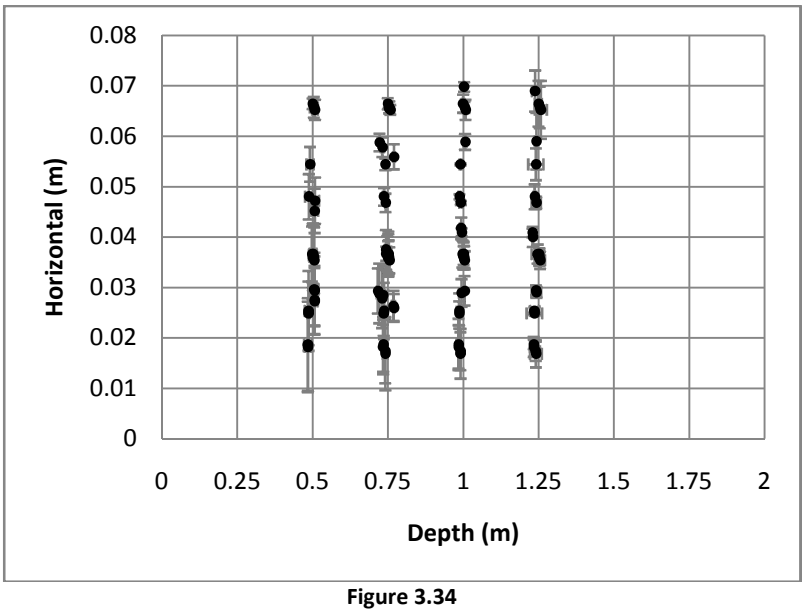

Figure 3.34
Horizontal Measured Location vs. IR Camera Location

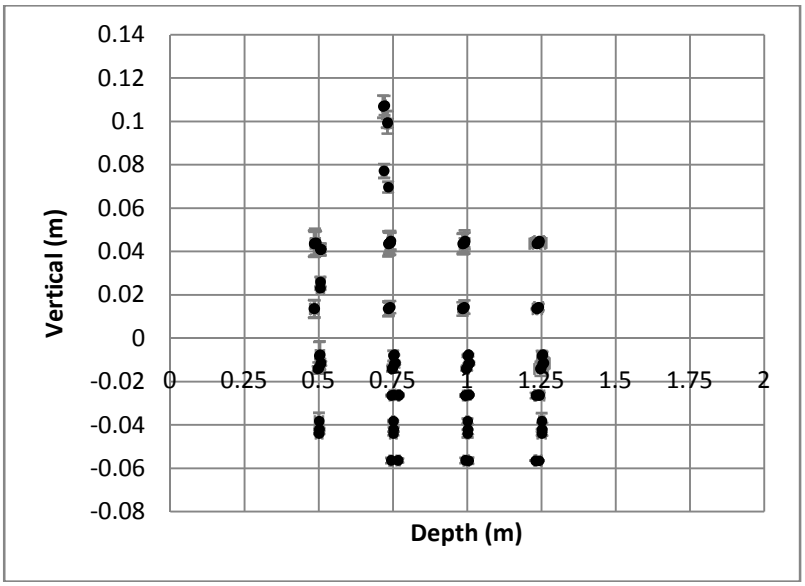

Figure 3.35
Vertical Measured Location vs. IR Camera Location

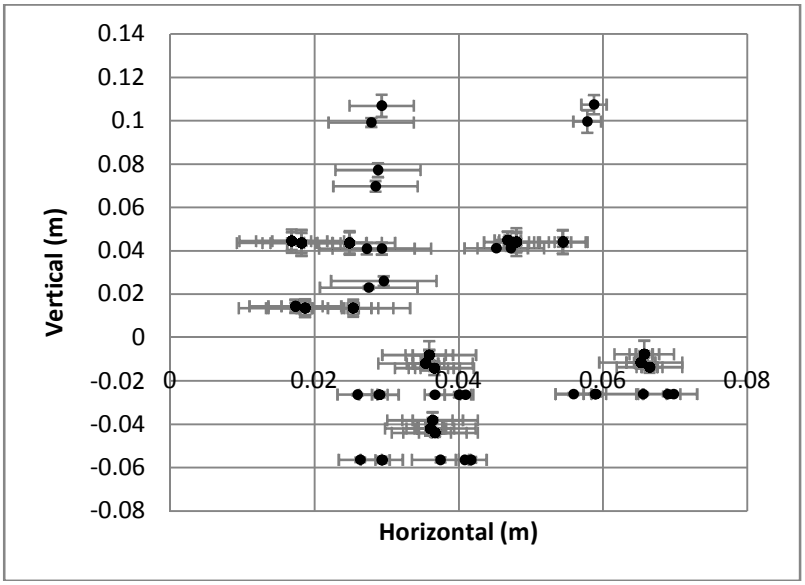

Figure 3.36
Horizontal Measured Location vs. Vertical Measured Location

3.5.2.3 Experiment 2.3: Maximum Roll, Pitch, and Yaw Angles

In the intended hand position measurement in VR simulations, the measurement system needs to be able to measure the yaw and pitch angles of the hand. In Experiment 1.3, the roll angle measurement was assessed using a single Camera and 2 LED sources. In this experiment, two parallel Cameras and a target with 3 LEDs were used. The goal was to determine the limits of the roll, pitch and yaw angles that the system could measure.

The experiment began by placing the LEDs in the frame with 10 mm spacing. Data was collected at a depth of 500 mm from the Wii Camera. However, beyond a depth of 500 mm, the Camera readings were not reliable. Therefore, the LED spacing was increased to 30 mm. A quick test showed that the Wii Remote could determine all three points at a depth of 1250 mm. Beyond this depth, the spacing needed to be increased. The equations used to calculate the angles are in Equations (3.11) through (3.14).

Rotational Matrix

$$\boldsymbol{R} = \begin{bmatrix} \boldsymbol{r_{11}} & \boldsymbol{r_{12}} & \boldsymbol{r_{13}} \\ \boldsymbol{r_{21}} & \boldsymbol{r_{22}} & \boldsymbol{r_{23}} \\ \boldsymbol{r_{31}} & \boldsymbol{r_{32}} & \boldsymbol{r_{33}} \end{bmatrix} \tag{3.11}$$

Roll equation

$$\boldsymbol{\beta} = \boldsymbol{atan^2}\left(\boldsymbol{r_{31}}, \sqrt{\boldsymbol{r_{11}}^2 + \boldsymbol{r_{12}}^2}\right) - \mathbf{90} \tag{3.12}$$

Pitch equation

$$\boldsymbol{\gamma} = -\boldsymbol{atan^2}\left(\frac{\boldsymbol{r_{32}}}{\boldsymbol{cos(\beta)}}, \frac{\boldsymbol{r_{33}}}{\boldsymbol{cos(\beta)}}\right) + \mathbf{90} \tag{3.13}$$

Yaw equation

$$\boldsymbol{\alpha} = \boldsymbol{atan^2}\left(\frac{\boldsymbol{r_{21}}}{\boldsymbol{cos(\beta)}}, \frac{\boldsymbol{r_{11}}}{\boldsymbol{cos(\beta)}}\right) - \mathbf{90} \tag{3.14}$$

The accuracies of the measured roll, pitch, and yaw angles are shown in Figure 3.37, Figure 3.38, and Figure 3.39. When comparing the error in these charts, there was far less error in roll compared to pitch and yaw. This is most likely due to the triangulation of the data points. In the case of roll measurements, the LEDs were directly facing the Cameras. The measurement of the yaw and pitch

angles were affected by the blob size of the IR LEDs detected by the Cameras. Therefore, if the yaw or pitch angle was too much, the bright blob seen by the Camera would shrink in size, rendering the measurement more inaccurate.

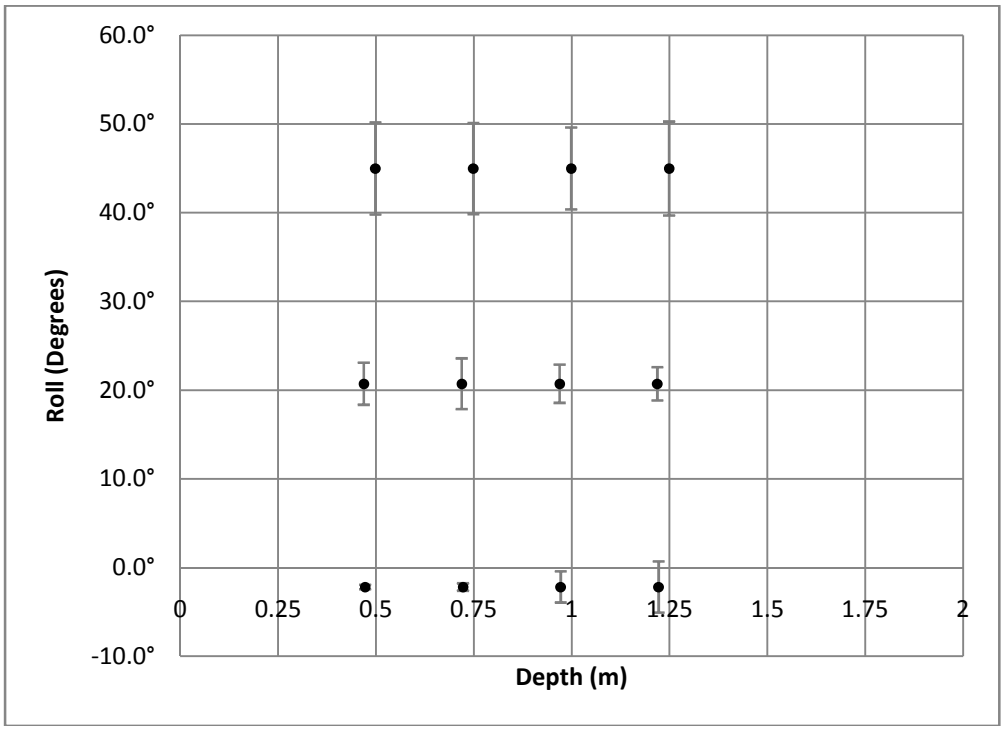

Figure 3.37
Roll Angle vs. Depth from Camera

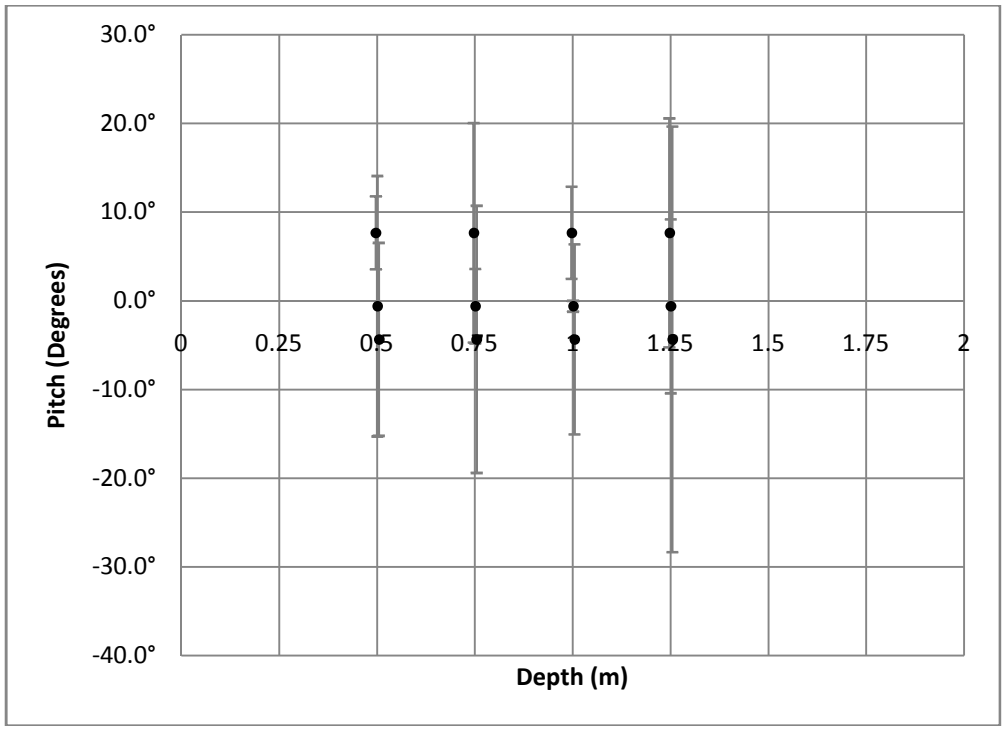

Figure 3.38
Pitch Angle vs. Depth from Camera

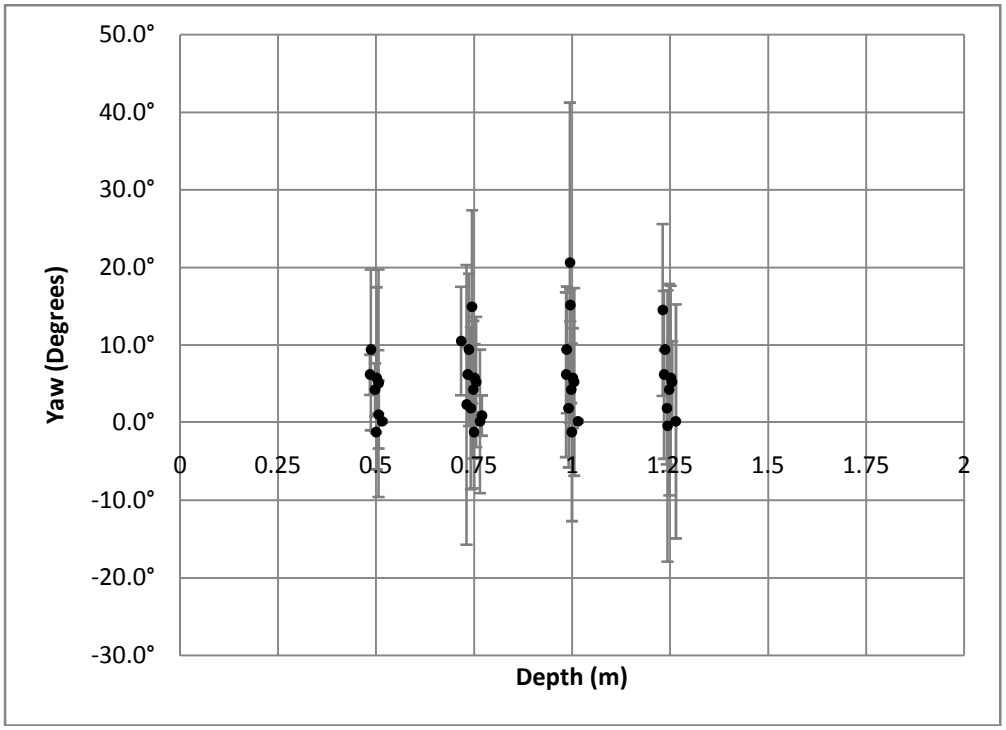

Figure 3.39
Yaw Angle vs. Depth from Camera

3.5.2.4 Freedom of Movement

The Freedom of Movement is a metric that attempts to quantify the size of the work volume that the Wii Remote can measure [4] (Figure 3.40). Equation (3.15) and Figure 3.41 describe the horizontal width of work volume (the Freedom of Movement).

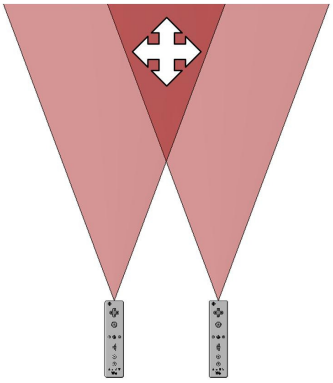

Figure 3.40
Freedom of Movement Diagram

$$x = 2tan\left(\frac{\theta}{2}\right) * y - \varsigma \qquad \textbf{(3.15)}$$

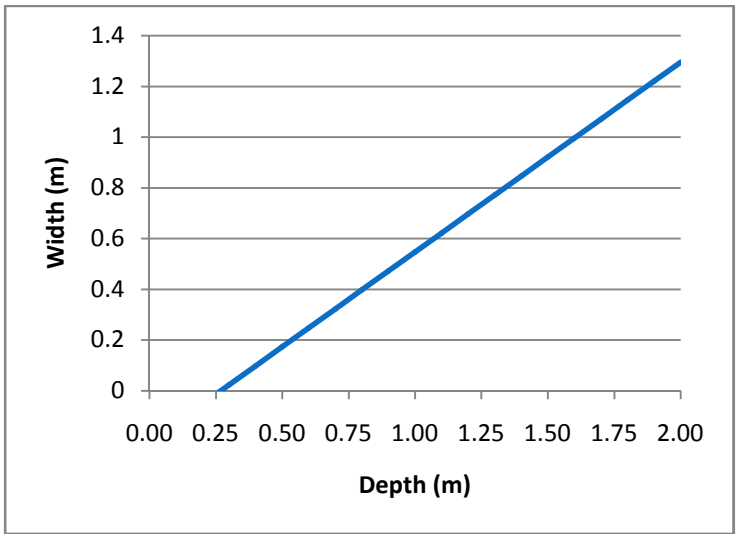

Figure 3.41
Freedom of Movement Available

3.5.3. Two Angled Wii Remotes

When the definition of the Freedom of Movement metric is examined, it can be seen that slightly rotating the two Wii Remotes towards each other may increase the resulting work volume. The primary goals of this set of experiments were to find (1) the optimal angle of the Cameras, (2) the resulting work volume, and (3) the measurement accuracy in this volume.

3.5.3.1 Wii Angle

Based on the data collected earlier, the most accurate regions of the workspace were closest to the Wii Remotes because of the increased Camera sensitivity. Analysis showed that the region of increased accuracy was between 0.5 m and 1.0 m away from the Camera, with 0.5 m being the most accurate. With this in mind, the Wii Remotes were angled inward until the greatest cross-sectional width was achieved at around 0.5 m depth from the Cameras. In Figure 3.42 and Figure 3.43, the dimensions were calculated using Equations (3.16) through (3.21c) and graphed in Figure 3.44.

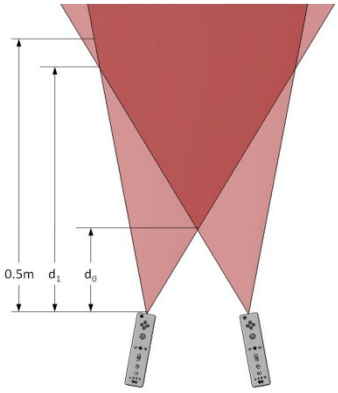

Figure 3.42
Depth Distances

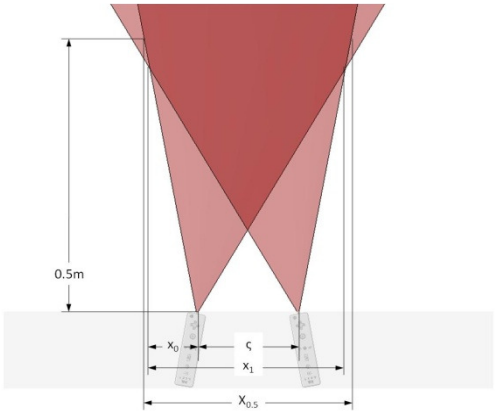

Figure 3.43
Horizontal Distances

$$\boldsymbol{\theta_1 = 20.5 - \theta} \quad \textbf{(3.16)}$$

$$\boldsymbol{\theta_2 = 20.5 + \theta} \quad \textbf{(3.17)}$$

Distance between Wii Remotes

$$\varsigma = \boldsymbol{200.61\ mm}$$

Wii Remote Merge Points

$$\boldsymbol{d_0 = \frac{\frac{\varsigma}{2}}{tan(\theta_2)}} \quad \textbf{(3.18)}$$

$$\boldsymbol{x_0 = \frac{\varsigma * tan(\theta_1)}{tan(\theta_2) - tan(\theta_1)}} \quad \textbf{(3.19)}$$

$$\boldsymbol{d_1 = \frac{x_0}{Tan(\theta_2)}} \quad \textbf{(3.20)}$$

Calculating the Width at 0.5 m

$$\boldsymbol{x_{0.5a} = 2 * \left(0.5 * tan(\theta_1)\right) + \varsigma} \quad \textbf{(3.21a)}$$

$$\boldsymbol{x_{0.5b} = 2 * \left(0.5 * tan(\theta_2)\right) - \varsigma} \quad \textbf{(3.21b)}$$

$$\boldsymbol{x_{0.5} = min(x_{0.5a}, x_{0.5b})} \quad \textbf{(3.21c)}$$

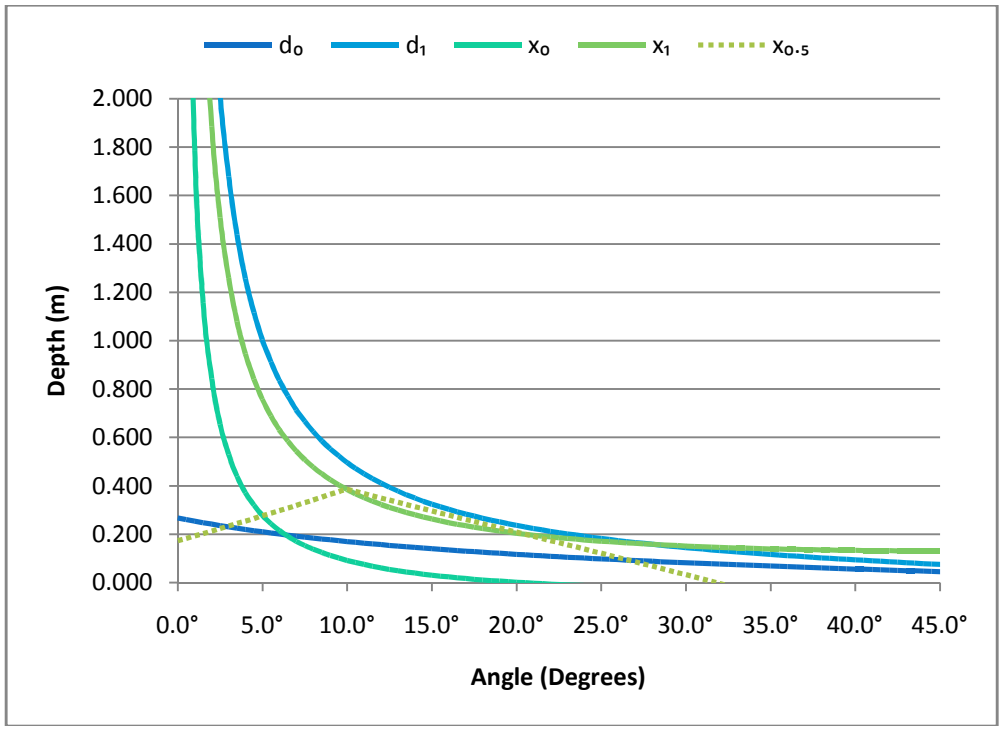

Figure 3.44
Camera Angle versus Depth

For consistency between this experiment and the previous ones, the horizontal distance of separation between the Cameras (ς) was kept the same as before. As seen in Figure 3.44, at about 10.0°, the cross-sectional width was greatest at a distance of 400-500 mm. When the Wii Remotes were parallel, the width was 173.3 mm. When the Cameras were rotated 10.0° towards each other, the width expanded to 386.9 mm. This is an increase of about 123% (Figure 3.45).

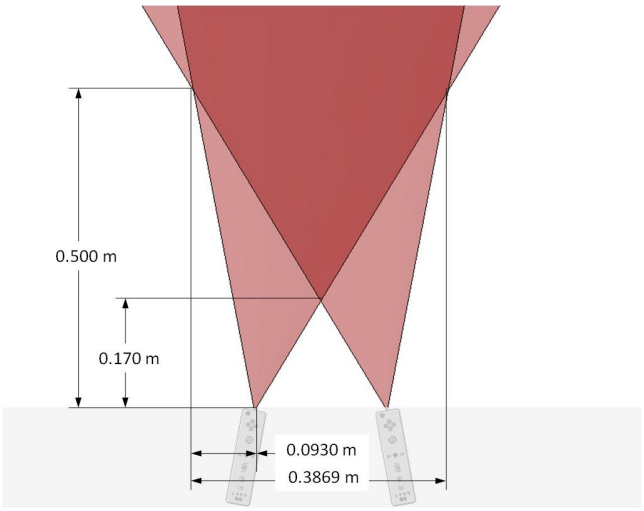

Figure 3.45
Final Rotated Wii Remote Design

Using the results of Experiment 2.1: LED Angle of Inclination, it was found that the closest the IR LED could be to the Wii Remotes, and still be seen by both Remotes, was about 214 mm (Figure 3.46).

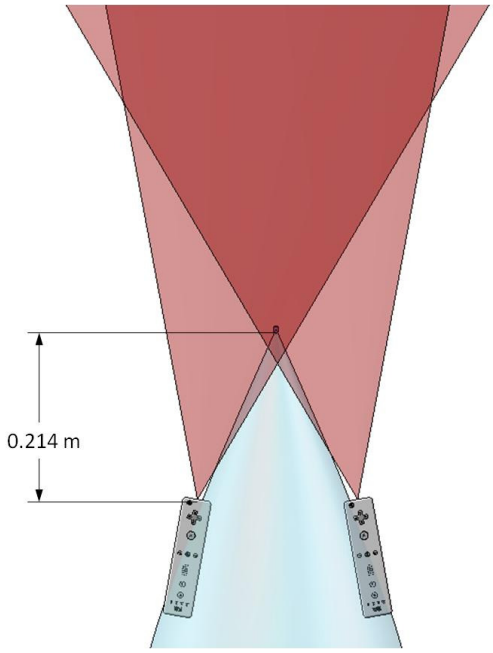

Figure 3.46
Minimum IR LED Depth with Rotated Wii Remote

3.5.3.2 Depth Analysis

There was very little that needed to be altered from the parallel Wii Remote experiment to the angled Wii Remote experiment. These modifications were limited to θ_1 and θ_2 as shown in Equations (3.22) and (3.23).

$$\boldsymbol{\theta_1 = tan^{-1}\big((0.5 - X_1) * h\big) - 10^{\circ}} \quad \textbf{(3.22)}$$

$$\boldsymbol{\theta_2 = tan^{-1}\big((0.5 - X_2) * h\big) + 10^{\circ}} \quad \textbf{(3.23)}$$

After gathering the initial set of data for this experiment, a large error was observed in the Y plane (Figure 3.47). Using the trend line shown in Figure 3.47, the error could be corrected by adding the computed value to the measured one from the Wii Remotes.

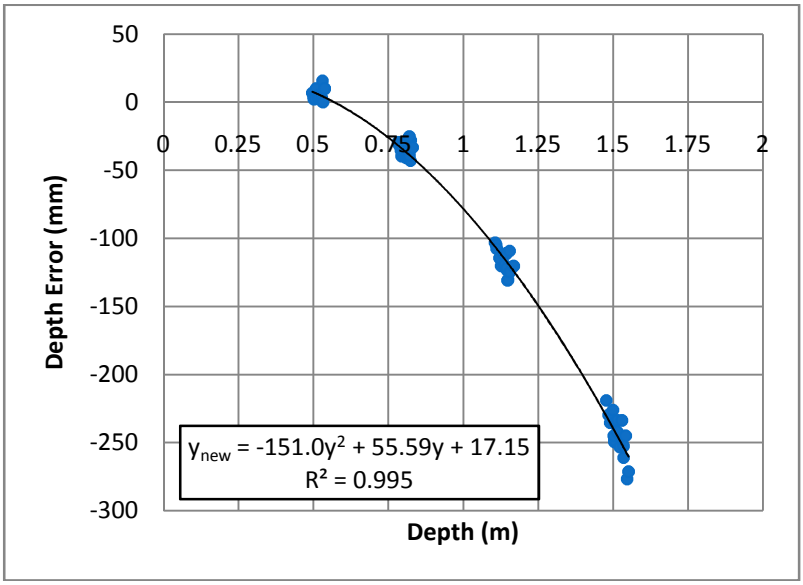

Figure 3.47
Depth Error

Trend Line Depth Recalculation

$$\boldsymbol{y_{new} = -151.0 * y^2 + 55.59 * y + 17.15} \quad \textbf{(3.24)}$$

Equation (3.24) reduced the error to values that were similar to previous experiments (Figure 3.48). As expected, error increased with depth from the Camera.

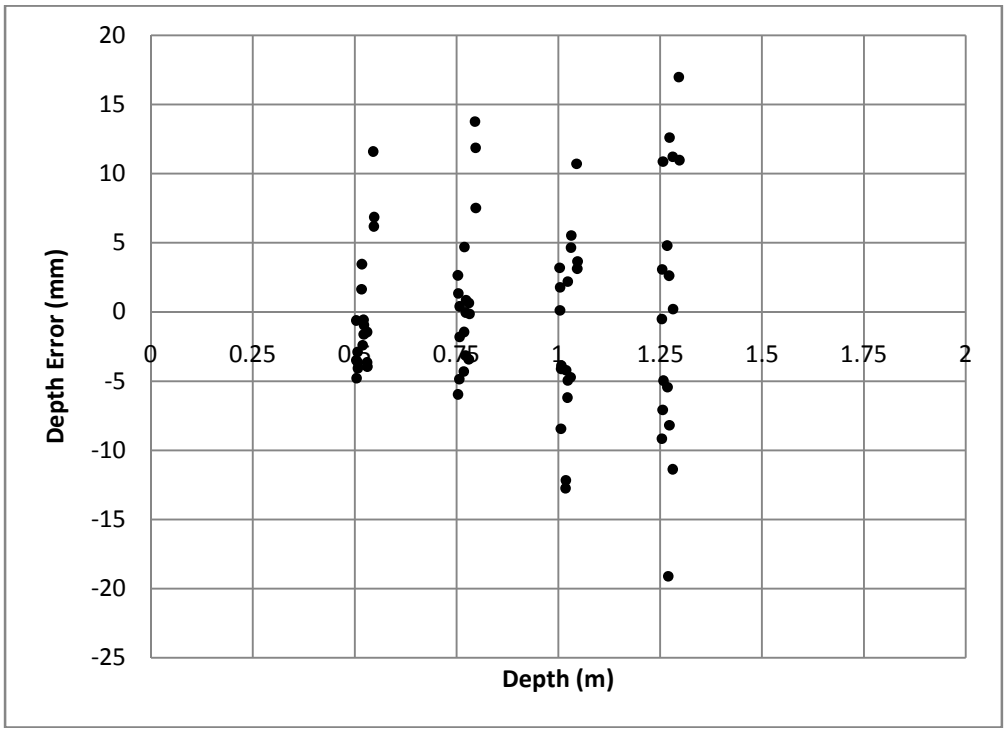

Figure 3.48
Depth Error Recalculated

The error recorded in the horizontal axis and vertical axis was similar to previous tests (Figure 3.49, Figure 3.50, and Figure 3.51).

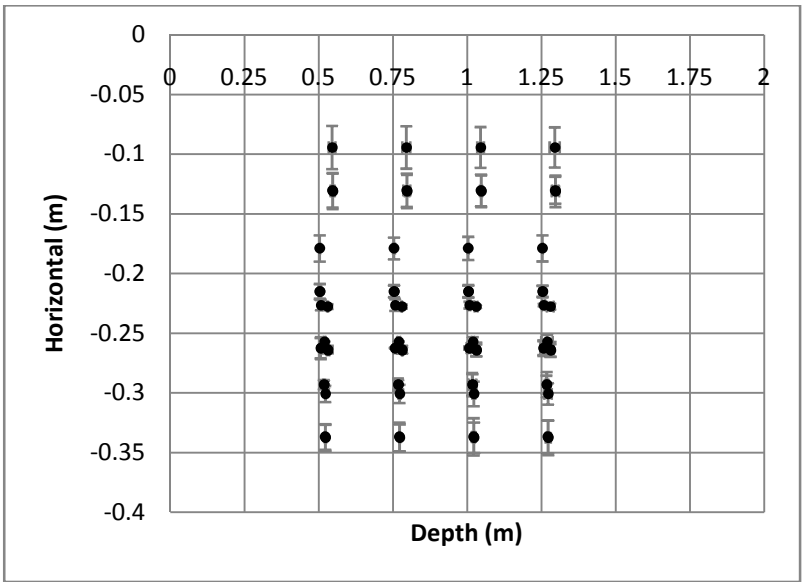

Figure 3.49
Horizontal Measured Location vs. IR Camera Location

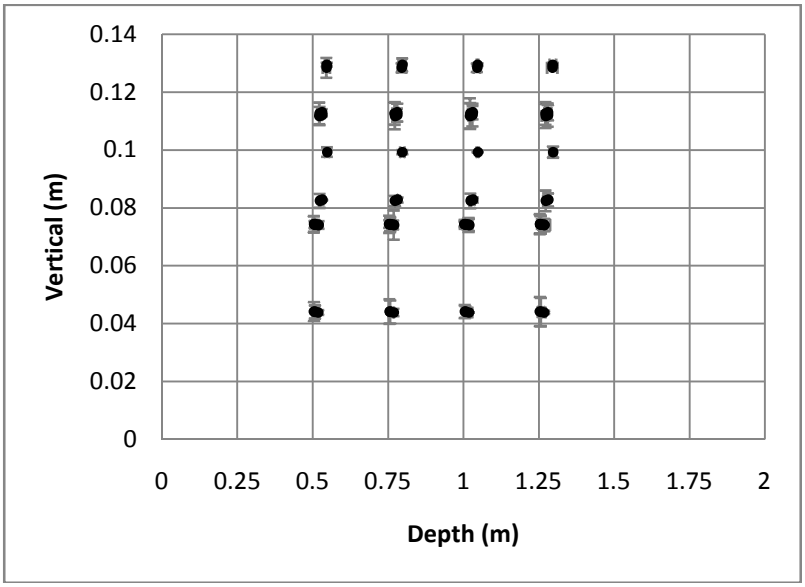

Figure 3.50
Vertical Measured Location vs. IR Camera Location

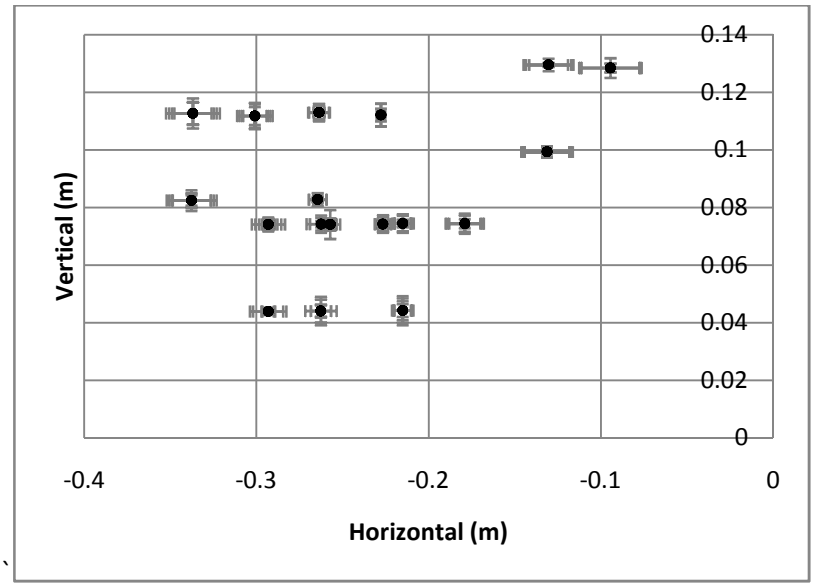

Figure 3.51
Horizontal Measured Location vs. Vertical Measured Location

3.5.3.3 Freedom of Movement

Part of the goal of this experiment set was to increase the Freedom of Movement and hopefully the accuracy within the workspace. Equations (3.25) through (3.27) describe the alterations to the Freedom of Movement value [4].

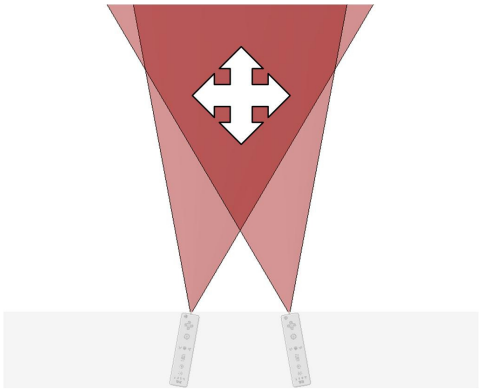

Figure 3.52
Freedom of Movement Diagram

Minimum Freedom of Movement Value

$$x_{min} = 2 * tan\left(\frac{\theta}{2} + 10°\right) * y - \varsigma \quad \textbf{(3.25)}$$

Maximum Freedom of Movement Value

$$x_{max} = 2 * tan\left(\frac{\theta}{2} - 10°\right) * y + \varsigma \quad \textbf{(3.26)}$$

True Freedom of Movement Value

$$x = min(x_{min}, x_{max}) \quad \textbf{(3.27)}$$

An increase in the Freedom of Movement was achieved between the depths of 0.5 m and 1 m as shown in Figure 3.53.

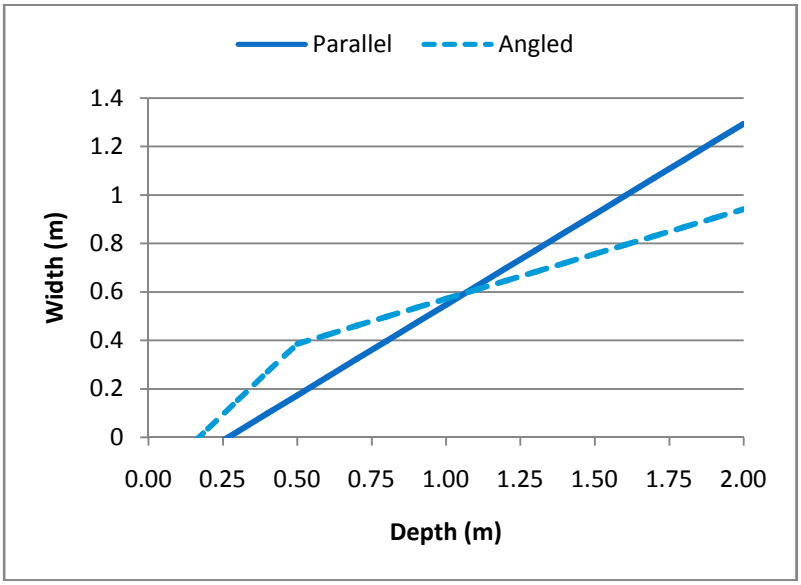

Figure 3.53
Freedom of Movement Comparison between Parallel and Angled Wii Remotes

3.6. Comparison to the Flock of Birds Sensor

The Flock of Birds system by Ascension is a popular measurement system in the virtual reality community for 3D position and orientation measurements. Table 3.3 shows the system specifications.

Specification	Flock of Birds	Nintendo Wii Remotes	
		Parallel	Angled
Tracking Range	±1.2m or ±3.05m	0.5m to 1.5m	0.5m to 1.5m
Angular Range	±180° Yaw & Roll, ± 90° Tilt	±20.5° Yaw, ±15.5° Tilt	±30.5° Yaw, ±15.5° Tilt
Static Accuracy			
• **Position**	1.8mm RMS	Depth: 7.5mm Horizontal: 3 mm Vertical: 2.5 mm	Depth: 5 mm Horizontal: 7.5 mm Vertical: 2.25 mm
• **Orientation**	0.5° RMS	Roll: 1.3° Pitch: 11.3° Yaw: 8.5°	(Not Tested)
Static Resolution			
• **Position**	0.5mm @ 30.5 cm	Horizontal: 0.66 mm Vertical: 0.66 mm @ 1 m Horizontal: 0.25 mm Vertical: 0.25 mm @ 30.5 m	(Not Tested)
• **Orientation**	0.1° @ 30.5cm	(Not Tested)	(Not Tested)
Update Rate	Up to 144 measurements/second	100 measurements/second	
Outputs	X,Y, Z positional coordinates and orientation angles, or rotation matrix		

Table 3.3
Technical Schematics Comparison [14]

There is a very significant cost difference between the Flock of Birds system and the Nintendo Wii method [15]. Comparison information has been accumulated in Table 3.4.

Cost	Flock of Birds	Nintendo Wii
Main Device		
	$1,385	(none)
Transmitter		
• **Short range**	$495	$5 For each IR LED (4 max)
• **Long range**	$650	
Sensors		
• **Short range**	$2,495*	$40 For each Wii Remote
• **Long range**	$7,845*	

*Discounts available for multiple orders

Table 3.4
System Cost Comparison
Flock of Birds vs. Nintendo Wii

CHAPTER 4

HAPTIC GLOVE DESIGN

This phase of the research involved preliminary design of a future glove that would accommodate the small actuators and the LED targets of the Wii Remote for hand position/orientation measurements in 3D. This portion was an auxiliary tangent of the whole but connects the two topics of 3D tracking (Chapter 3) and MR Brakes (Chapter 5). An initial CAD model of the glove was developed (Figure 4.1).

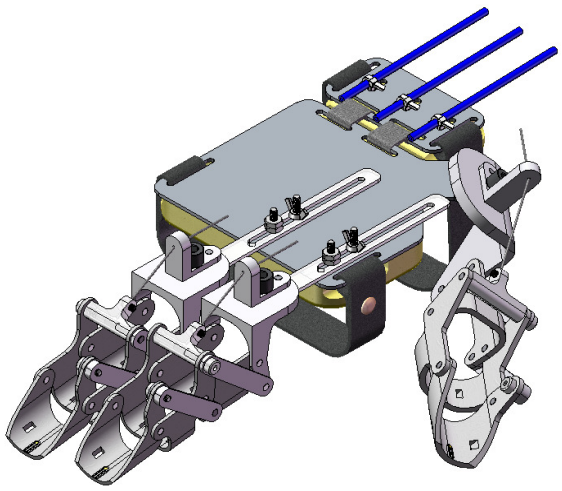

Figure 4.1
Haptic Glove CAD Model

4.1. Previous Designs

There have been several haptic glove designs completed at Washington State University Vancouver. They mainly consisted of an aluminum frame with a mechanical linkage system. One version of the haptic glove is shown in Figure 4.2. The bending of a finger extended or contracted a length of wires. It was by determining this change in wire length that the position of each finger's movement was calculated. Most of the joints had pin joints to reduce complexity. For the knuckle joint, this was not possible, so a curved slot was designed. After construction, it was found that the curved slots, although effective in their ability to pivot about the knuckle joint, tended to bind. In addition to this, the difference in hand dimensions between individuals and a fixed wrist were also analyzed and modified to allow for a more flexible fit.

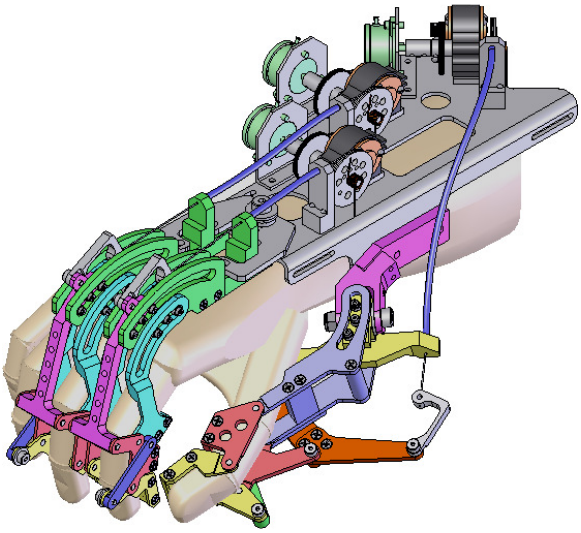

Figure 4.2
Previous Design [5]

4.2. Redesign of the Glove

Our redesign of the glove focused on three areas. The first was to make the movements more accurately match the actions of the user through a linkage design. The second was to lighten the glove. The third was to give the glove a more personalized fit for those with varied hand sizes.

4.2.1. Linkage System

The linkage system was originally designed by Conrad Bullion. He devised a method in which moving a single joint of a finger caused all the other joints of that finger to move synchronously (Figure 4.3). Using his method, a computer program was written to iterate through the possible variables to locate the most consistent solution for natural movement (Figure 4.4) [7].

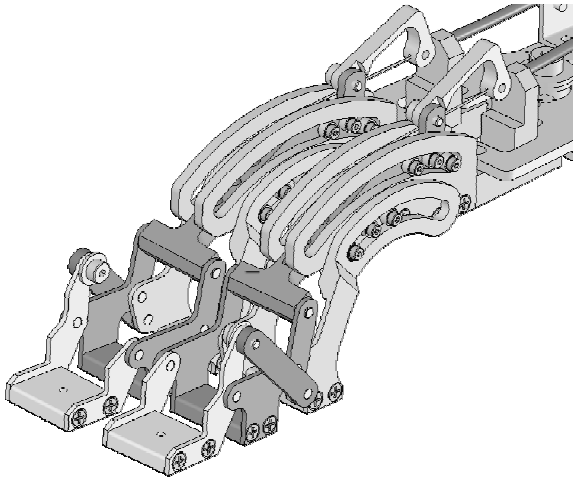

Figure 4.3
Old Linkage System

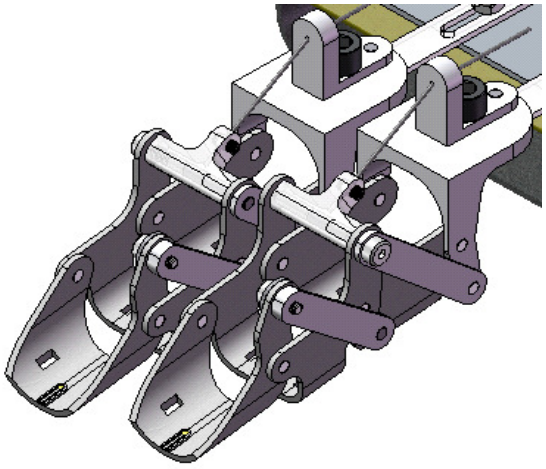

Figure 4.4
New Linkage System

The second part of the linkage system was the primary joint for the knuckles. In the old glove, there were three parts used along with twelve bearings for this joint (Figure 4.5). Although the movement was able to mimic the natural curvature of the knuckle, the joint was susceptible to repetitive binding. The combination of the bearings and unanticipated irregularities in the curve were the main source of this problem. A simplification of the joint postulated to remove this inherent

difficulty. In the new glove, the resulting joint was reduced to a single pin joint on both sides of the finger (Figure 4.6). This new joint was translated forward to avoid interference from the palm.

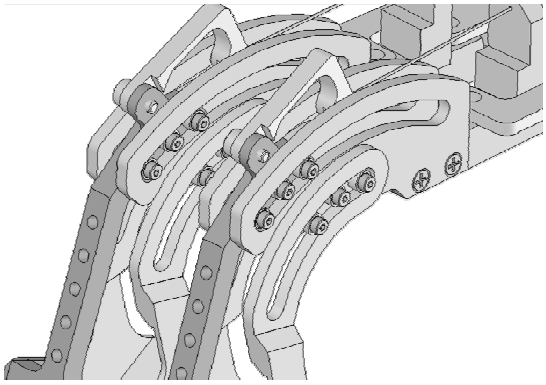

Figure 4.5
Old Knuckle Joint

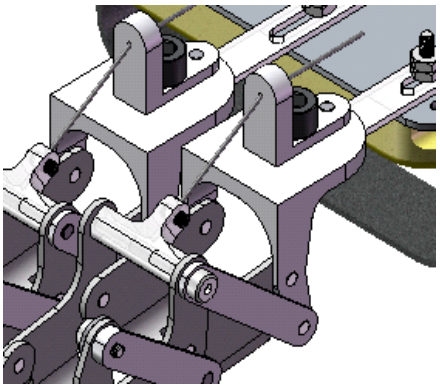

Figure 4.6
New Knuckle Joint

4.2.2. Weight Reduction Concepts

There were several options available for reducing the weight of the assembly. The first was to reduce the size of the attached frame. Making the assembly wireless would also assist in this goal. When the glove was connected to the computer by a cable, inadvertent limitations were created. These restrictions included a range of movement and the additional weight of the cables as the glove was lifted further from the ground. It was decided to make the frame out of $\frac{1}{16}$ inch steel to provide strength. For the finger assembly, a single part made from high strength plastic instead of the multiple aluminum parts was implemented. Simulations predicted that this new proposed glove will weigh less than 0.5 pounds. The actuators and sensors will be located on the user's shoulder to further reduce the total weight put on the hand.

4.2.3. Personalized Fit

To make the glove more comfortable to users, three steps were incorporated for fit. The first was to add curvature to each finger's mechanical support. This provided a close glove-like feel. The

second modification was to make the fingers adjustable by mounting the fingers to a sliding bar (Figure 4.7). By tightening thumb screws, the sliding bar locked the finger assembly in place.

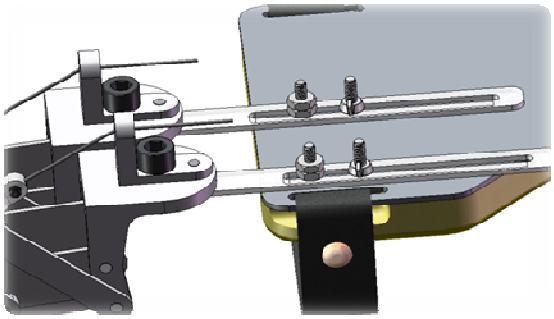

Figure 4.7
Adjustable Fingers

The final change was to the wrist assembly to provide flexibility in the wrist. In previous versions, the glove's main support extended from the knuckles to halfway up the forearm. A fix to this setup was to split the frame into two sections. The first was for the back of the hand, and the second was for the wrist itself. To connect the two, a nylon ribbon was used to provide a flexible joint. To attach all the supports to the user's arm, Velcro strips were used as in previous versions. One Velcro strip tightened across the user's palm, and another around the person's wrist (Figure 4.8).

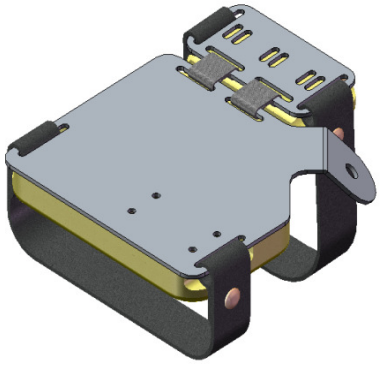

Figure 4.8
Adjustable Wrist

CHAPTER 5

LINEAR MR BRAKES USING A PERMANENT MAGNET

The long-term goal of our research is to develop a lightweight and powerful haptic glove. The main challenge in achieving this goal is the development of actuators that are small enough to be placed on the hand yet powerful enough to restrict or stop the motion of the fingers as the user grasps a virtual object. In this study, a small actuator was designed. The actuator uses magnetorheological (MR) fluid, a permanent magnet and a small motor. The ultimate goal is to use these actuators in the implementation of a future haptic glove.

5.1. Basic Design

Development of the linear MR Brake began with an analysis of the previous radial MR brakes and how they functioned. Alignment of the magnetic flux to be perpendicular to the movement of the shaft was crucial. No research papers on this specific subject were located to assist with the creation of the device. To further the progress of the design, there were two methods for adjusting the magnetic flux. The first was physically moving the permanent magnet towards the intended object, and the second was to adjust the rotation of the magnetic flux plane. The latter became the focus of the research because of the compactness and lighter weight of its design.

The design, as seen in Figure 5.1, contained five main parts. The first component was an aluminum shell which surrounds the whole to act as a Faraday Cage from stray minute magnetic fields.

The second element consisted of two iron cores that funneled the magnetic flux back and forth from the permanent magnet to the movable rod. The third and fourth items were the MR fluid that surrounded the rod and the rod itself. The final part was a rotatable cylinder that contained a neodymium magnet and two iron caps to complete the cylindrical shape. The caps acted as small connectors for the magnetic flux between the magnet and the iron cores. In this design, a servo could be attached to the cylinder with the magnet (Figure 5.2) to rotate the magnet.

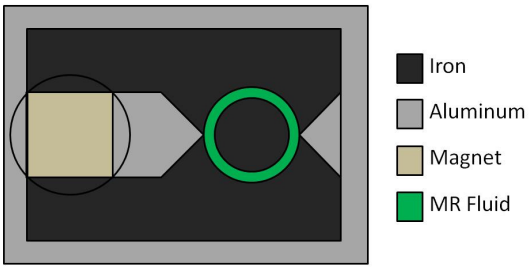

Figure 5.1
MR Brake Design

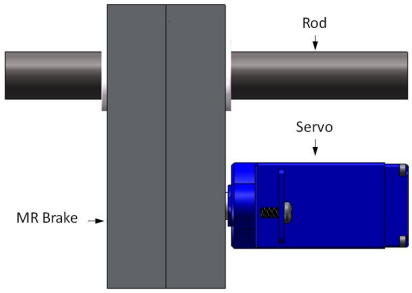

Figure 5.2
Top View Object Layout

As the cylinder rotates, a bottleneck is formed around one or both of the magnet's poles. In this instance, the maximum flux that flows through the MR fluid decreases following a sinusoidal path. The design was uploaded to a finite element analysis software. Results are shown in Figure 5.3.

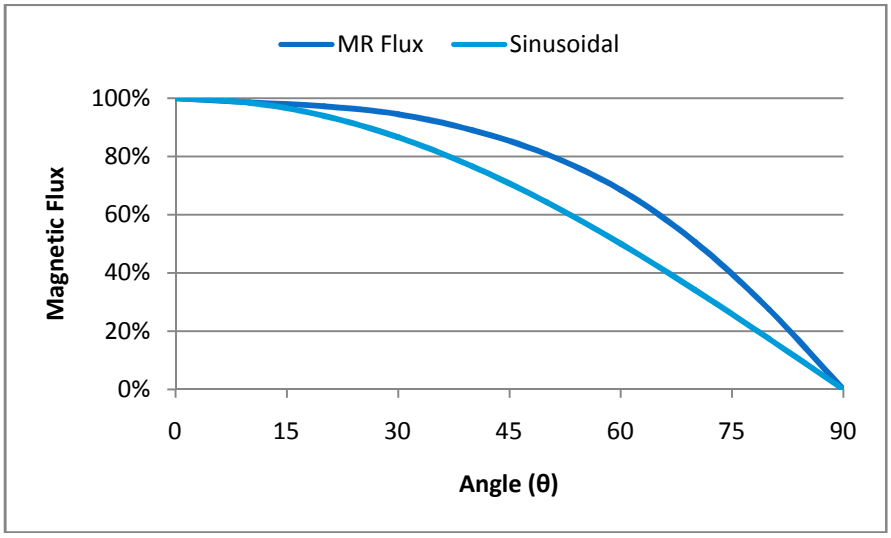

Figure 5.3
Angle vs. Magnetic Flux

5.2. Design Optimization

An optimization program was created to find the best possible values for the parameters involved in the design (Table 5.1 and Figure 5.4).

		Min (in)	Max (in)	Description
D_R	Rod Diameter	0.125	0.5	
D_G	MR Gap	0.001	0.125	
D_C	Core Distance	1.0	2.0	Natural flux range of the magnet
D_T	Brake Thickness	0.25	1.0	The greater the thickness, the greater the force that can be applied.
D_M	Magnet Width/Diameter	0.125	0.5	
θ	Convergence Angle	0°	60°	The angle that the magnetic flux follows converges to a single point.

Table 5.1
Design Optimization

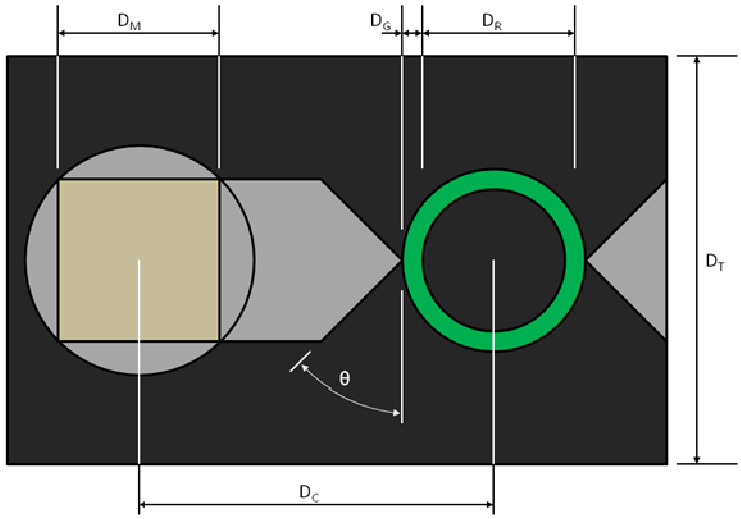

Figure 5.4
Brake Dimensions

Using an ANOVA statistical analysis, it was determined that D_R (Rod Diameter), D_G (MR Gap) and D_M (Magnet Width/Diameter) were the most dominant forces of the design (Table 5.2). The θ (Convergence Angle), D_T (Brake Thickness), or D_C (Core Distance) did not affect the results significantly.

Source	Degree of Freedom	Sum of Squares	Mean Square	F Value
D_M	1	0.245916	0.245916	39.60
D_G	1	0.079261	0.079261	12.76
D_M/D_G	1	0.007628	0.007628	1.23
D_M/D_R	1	0.003254	0.003254	0.52
D_G/D_R	1	0.003066	0.003066	0.49
D_C	1	0.001085	0.001085	0.17
θ	1	0.000764	0.000764	0.12
D_C/D_M	1	0.000622	0.000622	0.10

Table 5.2
ANOVA Results 1

Another ANOVA statistical analysis simulation was performed to narrow down the range of variables (Table 5.3). Using the program "Design Expert," it was determined that a magnet diameter of 0.5", an MR gap of $\frac{1}{64}$" and a rod radius range from 0.19" to 0.22" was best. The simulations showed that the optimal value was $\frac{7}{32}$" for the rod radius (Figure 5.5).

Source	Degree of Freedom	Sum of Squares	Mean Square	F Value
D_M	1	0.18	0.18	15.71
D_G	1	0.16	0.16	13.71
D_G^2	1	0.095	0.095	8.29
D_R^2	1	0.015	0.015	1.3
D_M^2	1	0.0015	0.0015	0.13
D_R	1	0.0005	0.0005	0.044
D_M/D_G	1	0.00017	0.00017	0.015

Table 5.3
ANOVA Results 2

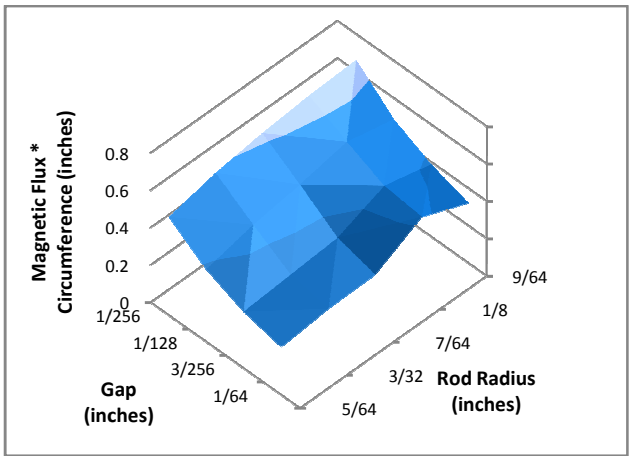

Figure 5.5
Magnetic Flux Strength

Even though this was the optimal radius, in practice it was too large. Having a rod that was almost half an inch in diameter would require a large amount of inertia to move. In addition, a brake with a force of nearly 20 N would be the resulting design which is far stronger than needed (Figure 5.6). A brake with a force between 10 and 15 N would work well. A rod radius of $\frac{1}{8}$" fits the criteria and would necessitate a force of about 12.5 N.

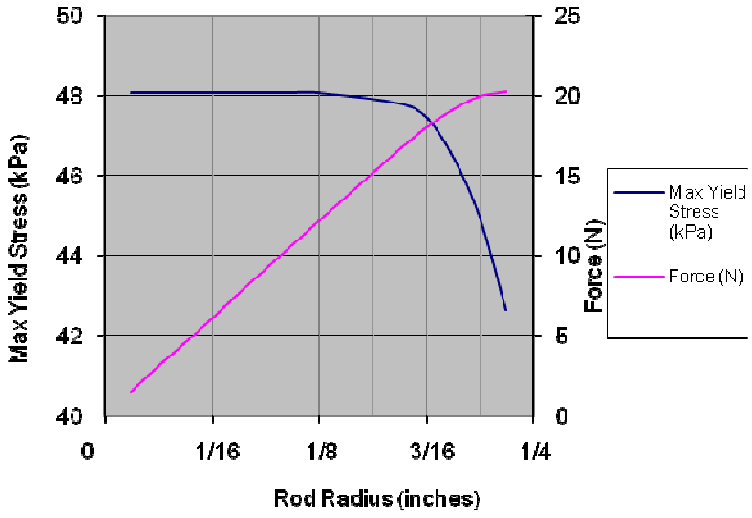

Figure 5.6
Predicted Brake Force

5.3. Final Design

The final dimensions of the Linear Magnetic Brake are shown in Table 5.4.

	Variable	Value
D_R	Rod Diameter	0.25"
D_G	MR Gap	$\frac{1}{64}$"
D_C	Core Distance	$\frac{11}{16}$"
D_T	Brake Thickness	0.5"
D_M	Magnet Width/Diameter	0.5"
θ	Convergence Angle	45°

Table 5.4
Final Optimized Dimensions

With the final values calculated, they were inserted into the simulation showing the magnetic flux intensity (Figure 5.7 and Figure 5.8). In Figure 5.8, the magnet is rotated 90° showing that there is no magnetic flux flowing through the MR fluid. The exploded design is shown in Figure 5.9.

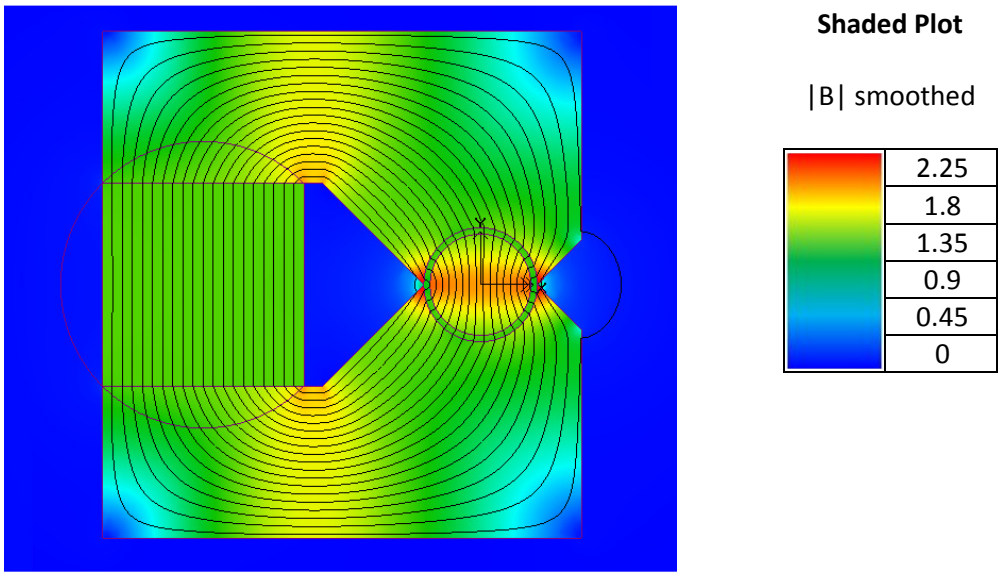

Figure 5.7
Final Magnetic Flux Shaded Plot

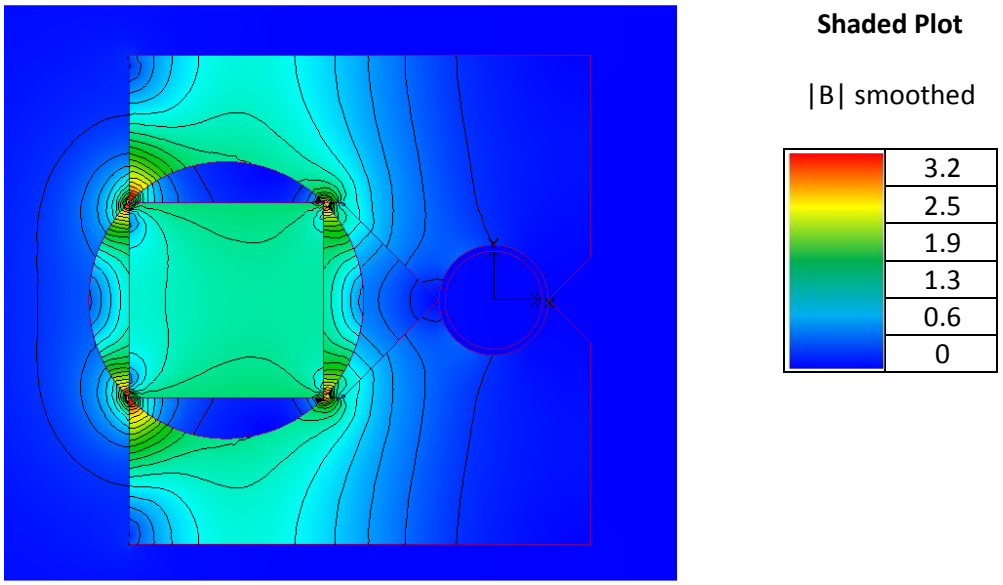

Figure 5.8
Final Magnetic Flux Shaded Plot with Magnet Rotated

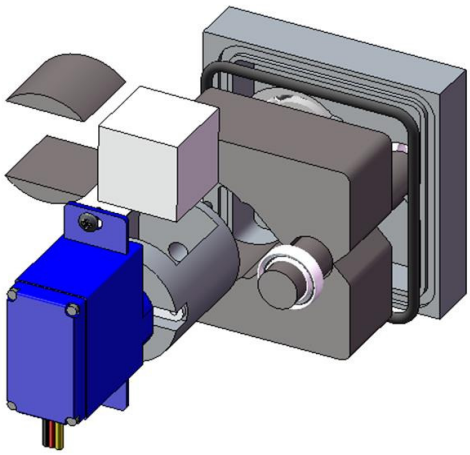

Figure 5.9
Final MR Brake Design Exploded View

(Front Cover Excluded)

CHAPTER 6

CONCLUSIONS

One of the challenges of developing a realistic, lightweight and powerful haptic glove is the real time measurement of user's hand position and orientation in 3D. The main emphasis of this study was on characterization of the Nintendo Wii Remote as a potential tracking system in virtual reality (Figure 6.1).

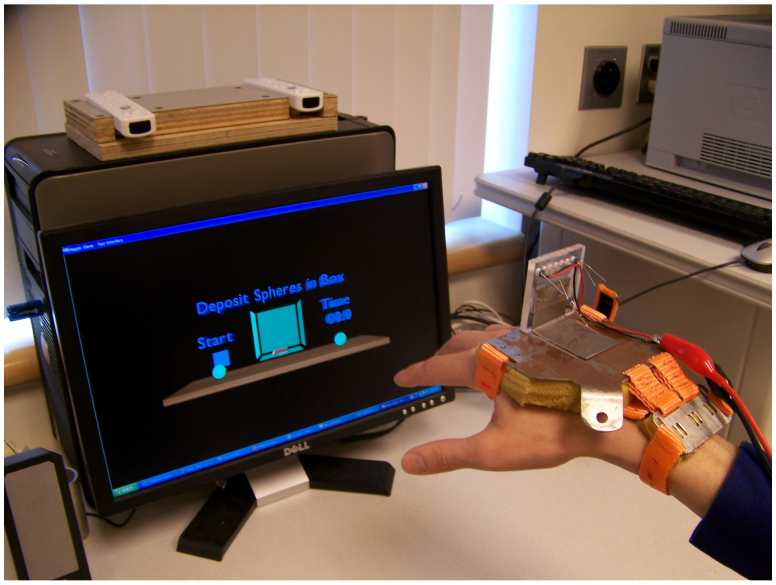

Figure 6.1
Nintendo Wii Remote Tracking the User's Hand Movements
For Virtual Reality Simulations

With this project, two other facets within haptic technology were developed. A new haptic glove design was proposed to fix the binding knuckle joint, lighten the assembly weight, and make the glove more comfortable for the user. A linear MR brake was designed using a rotating permanent magnet to control the force generated.

6.1. Characterization of the Wii Remote

The objective in Experiment Set 3 set out to accomplish two goals. The first was to increase the Freedom of Movement. This was accomplished between the depth of 0.25 m and 1.0 m (Figure 6.2).

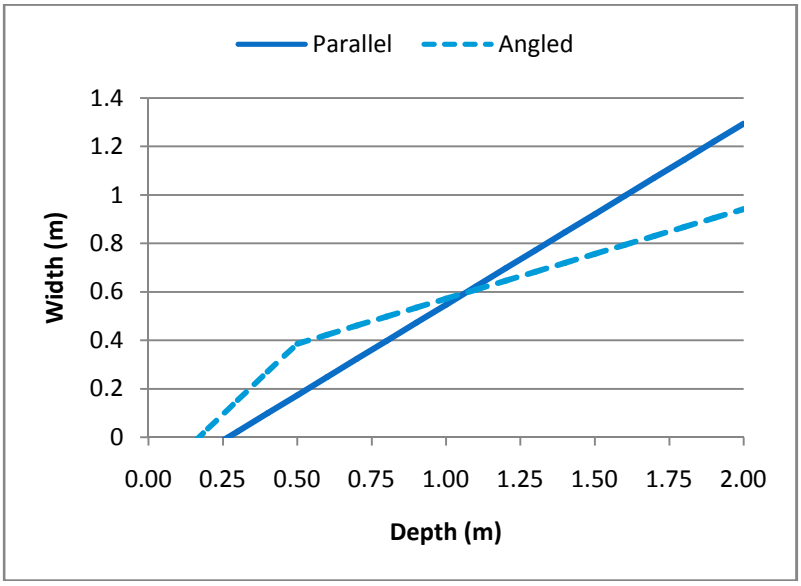

Figure 6.2
Freedom of Movement Comparison between Parallel and Angled Wii Remotes

The second goal of maintaining or increasing the accuracy fell short. The results associated with the Nintendo Wii Remote using Experiment Set 2 showed that the Wii Remote was fairly accurate calculating the depth from the Camera. In the horizontal axis, the error remained under 10 mm, while the vertical error fell below 6 mm. In Experiment Set 3, there was a non-linear distribution in the depth from the Camera calculation, so a polynomial equation had to be included to adjust the depth value. With this adjustment, the vertical error decreased to about 4 mm. Unfortunately, the horizontal error increased to 17 mm.

6.2. Haptic Glove Design

To further the progress of the haptic glove, several modifications were undertaken. The first change was to correct the binding within the knuckle joint of the thumb, index and middle fingers. This was accomplished by replacing the bearing and slot joint with a revolute joint. A modification to the mechanical linkage system was performed to correct any anomalies that would be generated.

The second change was to lighten the glove. This was achieved in two parts. First, different materials were used. The finger mechanisms were switched from multiple aluminum parts to plastic injection molds. The main support frame was switched from $\frac{1}{16}$" aluminum to $\frac{1}{32}$" stainless steel. Second, parts within the glove were reassigned to the shoulder to minimize the direct weight of the glove on the hand.

The last modification to the glove was to make it more comfortable for the user through improved fit. This included curving the finger support, making the finger position adjustable, and splitting the main support frame to enable a flexible wrist.

6.3. Linear MR Brakes Using A Permanent Magnet

To design a Linear MR Brake, several steps were taken. The magnetic flux flow was analyzed, a prototype structure formed, and the design optimized. A permanent magnet was used to generate the magnetic flux to maximize the efficiency. To adjust the magnetic flux intensity, a servo was chosen to rotate the magnet. As the magnet rotated, less and less magnetic flux flowed through the MR fluid, reducing the force generated. The final design allowed for a 0.25" diameter rod with a 0.5" cubed neodymium magnet as the source. Because of time limitations, the brake could not be constructed nor subsequent versions refined.

BIBLIOGRAPHY

[1] An, J., & Kwon, D.-S. (2008). Five-Bar Linkage Haptic Device with DC Motors and MR Brakes. Journal of Intelligent Material Systems and Structures OnlineFirst , 1-11.

[2] Lee, J. C. (n.d.). Retrieved 2009, from Johnny Chung Lee - Projects - Wii: http://johnnylee.net/projects/wii/

[3] Chow, Y.-W. (2009, February). 3D Spatial Interaction with the Wii Remote for Head-Mounted Display Virtual Reality. Wold Academy of Science , 38.

[4] Wronski, M. P. (2008, October). Design and Implementation of a Hand Tracking Interface using the Nintendo Wii Remote. Department of Electrical Engineering, University of Cape Town .

[5] Bullion, C. (2007). Haptic glove for distributed finger force feedback in virtual reality. MS thesis, School of Engineering and Computer Science, Washington State University,Vancouver, WA.

[6] Choi, T.-Y., Lee, J.-Y., & Lee, J.-J. (2006). Control of Artificial Pneumatic Muscle for Robot Application. International Conference on Intelligent Robots and Systems , 4896-4901.

[7] Dazkir, A. G. (2008). Active Control of a Distributed Force Feedback Glove for Virtual Reality Environments. Pulman, WA: Washington State University.

[8] Li, C., Tokuda, M., Furusho, J., & Koyanagi, K. (2009). Research and Development of the Intelligently-Controlled Prosthetic Ankle Joint. International Conference on Mechatronics and Automation (pp. 1114-1119). Luoyang, China: IEEE.

[9] Nintendo. (2009). What Is Wii? at Nintendo :: Wii. Retrieved May 18, 2009, from Nintendo: http://www.nintendo.com/wii/what

[10] Wimmer, R., Boring, S., & Müller, J. (2008*). Tracking the Wiimote in 3D using ARToolkit. University of Munich . Munich, Germany.

[11] Corporation, I. (2008). BlueSoleil. Retrieved from http://www.bluesoleil.com/

[12] RenEvo Software and Designs. (2008). Retrieved from http://www.renevo.com/

[13] gl.tter. (2009, 7 6). Retrieved from - WiiYourself! - gl.tter's native C++ Wiimote library.: http://wiiyourself.gl.tter.org/

[14] Corporation, A. T. (2009). Flock of Birds. Retrieved May 18, 2009, from Ascension Technology Corporation: http://www.ascension-tech.com/docs/Flock_of_Birds.pdf

[15] Inition. (n.d.). Retrieved from http://www.inition.co.uk/inition/product.php?URL_=product_mocaptrack_ascension_flockofbirds&SubCatID_=18&Tab=prices

APPENDIX

A. INSTRUMENT SETUP

Figure A.1
LED Frame for Experiment Set 1

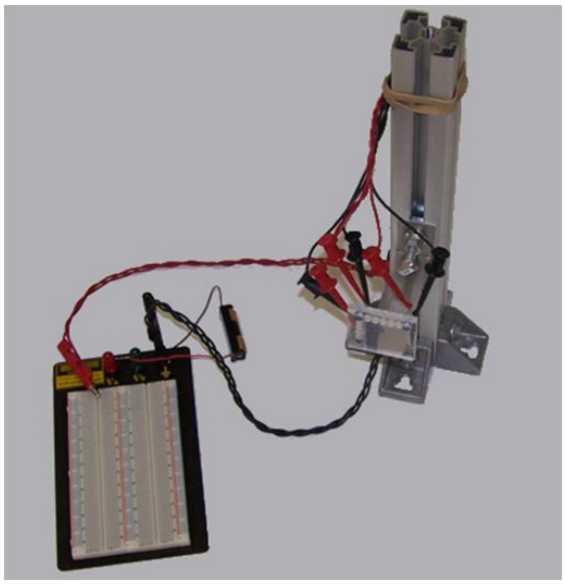

Figure A.2
LED Frame for Experiment Sets 2 and 3

Figure A.3
Typical Wii Remote Setup

Figure A.4
Elevated Wii Remote Setup

B. CODE MODIFICATION

Code 1 - Wii Yourself! Modification

This is a section of the code starting from line 318 to 353 deals with displaying the IR location that the Camera returns. The highlighted area in line 349 is where the only change was made. The entirety of the code can be found in the file "Demo.cpp" from "WiiYourself!_1.01a.zip" (gl.tter, 2009)

```
318:         // IR:
319:         CYAN ; _tprintf(_T("       IR:"));
320:         WHITE; _tprintf(_T("  Mode %s  "),
321:             ((remote.IR.Mode == wiimote_state::ir::OFF     )? _T("OFF  ") :
322:              (remote.IR.Mode == wiimote_state::ir::BASIC   )? _T("BASIC") :
323:              (remote.IR.Mode == wiimote_state::ir::EXTENDED)? _T("EXT. ") :
324:                                                               _T("FULL ")));
325:         // IR dot sizes are only reported in EXTENDED IR mode (FULL isn't supported yet)
326:         bool dot_sizes = (remote.IR.Mode == wiimote_state::ir::EXTENDED);
327:
328:         for(unsigned index=0; index<4; index++)
329:             {
330:             wiimote_state::ir::dot &dot = remote.IR.Dot[index];
331:
332:             WHITE;_tprintf(_T("%u: "), index);
333:
334:             if(dot.bVisible) {
335:                 WHITE; _tprintf(_T("See        "));
336:                 }
337:             else{
338:                 RED  ; _tprintf(_T("Not seen   "));
339:                 }
340:
341:             _tprintf(_T("Size"));
342:             if(dot_sizes)
343:                  _tprintf(_T("% 3d "), dot.Size);
344:             else{
345:                 RED; _tprintf(_T(" n/a"));
346:                 if(dot.bVisible) WHITE;
347:                 }
348:
349:             _tprintf(_T("  X %.6f  Y %.6f\n"), dot.X, dot.Y);
350:
351:             if(index < 3)
352:                 _tprintf(_T("                          "));
353:             }
```